Miocene Central Volcanoes, NW New South Wales: Genesis over a Lithospheric Cavity (?)

F. Lin Sutherland[1]
with illustrative contributions by B.E. Cohen[2] and M.B. Duggan[3].

[1]Australian Museum, 1 William Street, Sydney, NSW 2010 (Lin.Sutherland@austmus.gov.au);
[2]School of Geographical and Earth Sciences, University of Glasgow, Scotland, G12 8QQ, UK;
[3]519 Mulquinneys Road, Braunstone, NSW 2460

Published on 27 November 2019 at https://openjournals.library.sydney.edu.au/index.php/LIN/ind

Sutherland, F.L. (2019). Miocene central volcanoes, NW New South Wales: genesis over a lithospheric cavity (?). *Proceedings of the Linnean Society of New South Wales* **141,** S85-S114.

Basalt fields and central volcanoes form a curved south-migrating trace through NW New South Wales. A segment of East Australian intraplate volcanism, it traces Australia's northern plate motion north over a mantle plume system. This created the western New England basalt field (24 – 21 Ma), Nandewar central volcano (19 – 18 Ma), Warrumbungle central volcano (18 – 15 mya), Mount Canobolas central volcano (13 – 11 Ma) and minor alkaline eruptions near Oberon (10 – 9 Ma). This 'boomerang-shaped' segment initially swelled south-westerly with increasing mantle melting and basaltic evolution. After initial fluid basaltic outpourings in New England, it formed two large central volcanoes along its outward curve before bending southerly to form a smaller central volcano and a scattered tail of small late-eruptions. This volcanic trace did not match Australia's linear plate motion trend between 24 – 9 Ma. Neither did it correspond with adjacent plume trend seen in the leucititic lavas to the west, the coastal NSW plume volcanoes and Tasman Sea submarine plume chains to the east. Recent seismic tomography has revealed 'cavities' within the underlying lithosphere-asthenosphere boundary (LAB). The anomalous NW New South Wales plume upwelling underwent diversion by its interaction along the western edge of a LAB 'cavity'.

Manuscript received 10 June 2019, accepted for publication 1 October 2019.

KEY WORDS: age-dating, basalt fields, Cenozoic volcanism, central volcanoes, East Australia, lithospheric cavity, magmatic fractionation, mantle melting, plate motion, plume trace.

INTRODUCTION

This paper surveys Miocene volcanic rocks, their distribution, age, petrology, genesis, tectonic setting, geomorphic development, and features of general interest within north-western New South Wales. It is based on a presentation given at the 2018 Linnean Society of NSW on this theme at Coonabarabran, 25-26 September, 2018. The symposium also explored further relationships between geology, flora, fauna and fires, which were not pursued in this volcanic survey. The Symposium presentation was greatly enhanced by inclusion of extra material in the form of images of volcanic features and geological diagrams, particularly by Dr Ben Cohen, from his 2007 PhD thesis study, School of Physical Sciences, University of Queensland, and by Dr Morrie Duggan, from his studies and writings on the area, when employed at the Australian Geological Survey Organisation, now Geoscience Australia, Canberra, ACT. Many of these illustrations are included in this paper, with the permission and acknowledgement of the contributors, and add greatly to its illustrative content. Some volcanic content in this study appeared in a previous Linnean Society of New South Wales Symposium volume, on Geodiversity, Geoheritage and Geotourism, (Sutherland 2011). Those parts related to NW New South Wales volcanic areas, however, are revisited and updated with further relevant literature.

Geological setting

Eastern Australia has an extensive record of intraplate basaltic volcanism. Its latest prolonged cycle has continued in quasi-continuous mode for ~ 100 Ma, after initial early Cretaceous break-up events at ~ 125 Ma split Australia and New Zealand (Matthews et al. 2016 a, b). This episode initiated widespread elevated heat flows, leading to volcanic activity and

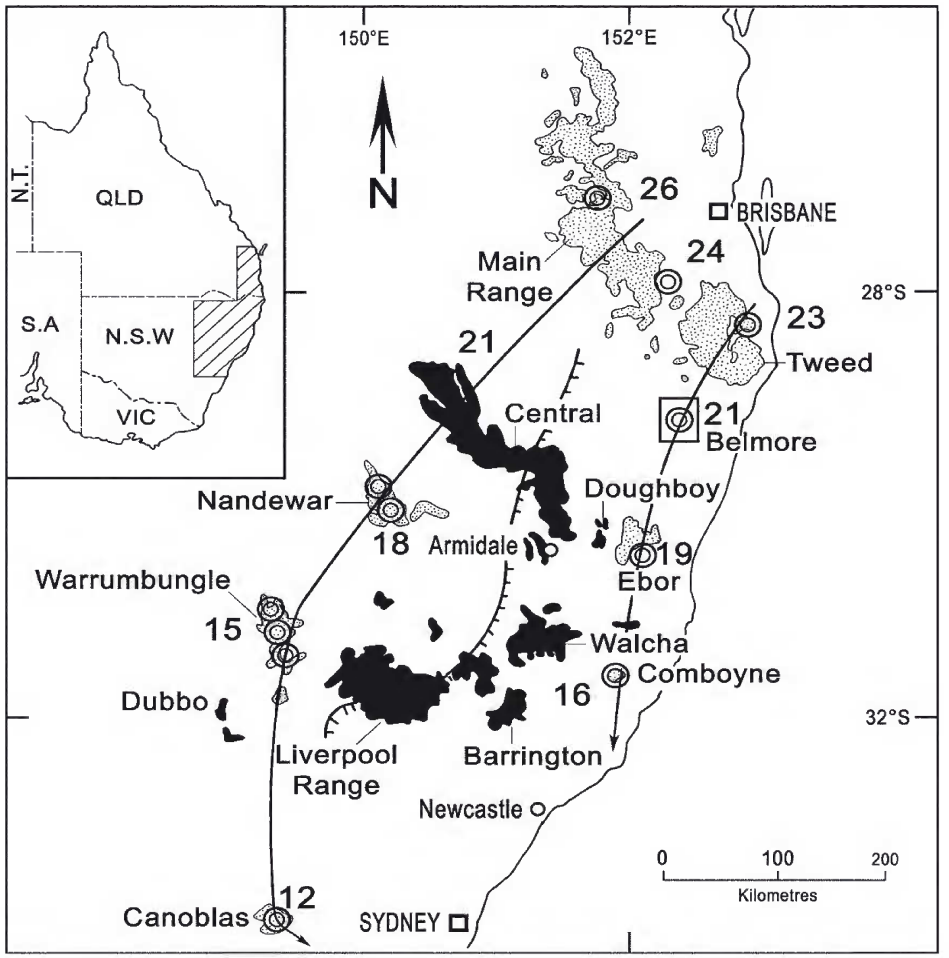

Figure 1. Distribution of central volcanoes (stippled areas) and basalt lava fields (black areas), Qld – NSW 26 – 36o S. Map shows main ages in Ma (based on available Ar – Ar and K- Ar ages), general age-progressive trends (arrowed lines) and western edge of the Sydney Basin (hatched line) The Belmore central volcano is outlined by a box to indicate its unusual silicic nature. The diagram is modified from Sutherland et al. (2005).

sea floor spreading events that dismembered the Gondwa margin into fragmented continental slivers (Higgins et al. 2015). The disruptions led to the rise of long-term asthenosphere-derived magmatic plume systems that developed migratory 'hot spot' volcanic chains over migrating lithosphere (Johnson 1989; Sutherland 2003; Sutherland et al. 2012; Cohen et al. 2013; Jones et al. 2017). Three types of volcanic fields were initially distinguished within eastern Australian volcanism, basaltic lava fields, central volcanoes which include both basaltic and evolved felsic components, and rarer leucititic lavas (Johnson 1989). The latter two types were associated with migratory plume-related activity, while basaltic lava fields were considered more random rift-related melting events. Later studies, however, have identified basaltic lava fields that appear to be associated with the migratory plume-derived fields (Sutherland 2003; Jones et al. 2017). The main NW New South Wales Miocene volcanic fields include basaltic lava fields, some plume-related, and well developed central volcanoes (Fig. 1), while age-progressive leucititic migratory volcanoes are confined to outer western fringes (Cohen 2007; Hansma and Tover 2018).

The term 'Volcanoes of Northwest New South Wales' used in the Coonabarabran Symposium needs definition here, as some volcanoes are variously designated north-eastern or central NSW in previous literature. This study covers the migratory Miocene age-linked North West NSW volcanic fields mapped west of Inverell (Brown and Stroud 1997; Vickery et al. 2007), and to the south-east includes the large Nandewar Range and Warrumbungle Range central volcanoes, all of which fall within the Brigalow Belt South Bioregion (Dawson et al. 2003). The lesser-sized Canobolas central volcano and minor Abercrombie basalt field (Pogson and Watkins 1998), however, lie south of the Brigalow Belt South Bioregion (Dawson et al. 2003). The fields overall extend between 149° 30'– 151° E and 29° – 33° 45'S. The Brigalow Belt South Bioregion also covers the eastern voluminous Oligocene-Eocene Maybole and Liverpool Range basaltic shields (up 1000 m in thick; Johnson 1989; Middlemost 2013), which are not considered here.

The feeder systems for the described migratory volcanoes penetrated a range of crustal basement units (Pogson and Watkins 1998; Dawson et al. 2003; Vickery et al. 2007). The underlying Paleozoic basement includes parts of the Lachlan and New England fold-belts (Glen 2013; 2015). The fold-belt rocks underlie an unconformity below late Permian mafic rocks and the following sedimentary beds of Gunnedah Basin (Ward and Kelly 2013). Westward, these beds are overlapped by late Triassic-Jurassic-early Cretaceous deposits of the Surat Basin.

The western New England basalt field (Fig. 2), was re-named the Delungra Volcanic Suite by Vickery et al. (2007). It includes older flows and plugs northwest of Inverell, which transgress Jurassic Surat Basin beds. West of Inverell younger lavas overlie the older basalts and were erupted from plugs that ascended through the early Permian Bundarra Batholith in the New England Fold Belt (Vickery et al. 2007). Smaller separate basalt fields around Bingara overlie Devonian-Carboniferous beds of the New England Fold Belt. The Delungra Volcanic Suite flows buried alluvial deposits of the Miocene drainage (Fig. 3), which carried unusual diamonds of unknown source (MacNevin 1977; Meyer et al. 1997; Barron et al. 2008).

Nandewar central volcano shows complex relationships to the underlying geology (Dawson et al. 2003). The northern part volcanics both intruded and overlie dissected Gunnedah and Surat Basin beds, although its northern nose volcanics overlie Cretaceous marine beds. Basaltic lavas in its northeastern extent overlie Cenozoic alluvial gravels, sands and silts. The central and southern parts of the volcano intrude through and overlie thrust-faulted Devonian and Carboniferous fold belt beds to the east side. Its west side largely overlies a dissected terrain of basal Permian mafic volcanic rocks and Permian-Triassic sedimentary beds within the Gunnedah Basin. In places, Nandewar extrusions overlie eroded sills of teschenite, an analcime-bearing dolerite. These are unrelated to Nandewar Volcano and were dated at 198 ± 2 Ma (Cohen 2007). Small basaltic flow remnants of Nandewar Volcano's original outreach continue along a N-S length of 120 km and an E-W width of 75 km (Geological Drive across the Nandewar Volcano. Bob and Nancy's Geotourism Site: http://ozgeotours.yolasite.com/ ; accessed 26/09/2019).

Many eruptive units of Warrumbungle Volcano are now remapped in greater detail (Troedson and Bull, 2018). Most overlie Jurassic sedimentary beds of Surat Basin, largely the braided stream deposits, but in places extend over mid-Jurassic alluvial and lake deposits (Dawson et al. 2003). The north western edge of the volcanic apron, however, rests on upper late Jurassic to early Cretaceous stream and coastal deposits. The feeder system in the central vent ascended into the Surat Basin sequence through the underlying Lachlan Fold Belt. Flows entered former radial drainages and extended flows travelling SSE intersected and infilled a former SW channel of Castlereagh River, diverting the river farther south (Dawson et al. 2003).

The rise and fall of Canobolas Volcano through growth and erosion in relation to the surrounding geology and regolith is outlined in Chan (2003). The feeder system erupted through the Lachlan Fold Belt and its outflowing lavas descended into drainages cut extensively in weathered plateau surfaces. In places, lavas flowed over Surat Basin beds infilling radial drainages to the northeast and reached exposed Bathurst Granite to the southeast.

Young zircon grains appear in alluvial deposits adjacent to basalts in the Abercrombie province (Sutherland 1993). These deposits lie ESE well beyond the older Canobolas eruptive apron. They suggest minor eruptions around Oberon after cessation of Canobolas activity.

VOLCANIC FIELDS, GEOCHRONOLOGY AND PETROLOGY

Delungra Volcanic Suite

Four separate areas of eruption were mapped within the basaltic suite (Fig. 4). These comprise two areas of largely silica-saturated tholeiitic basalts, the

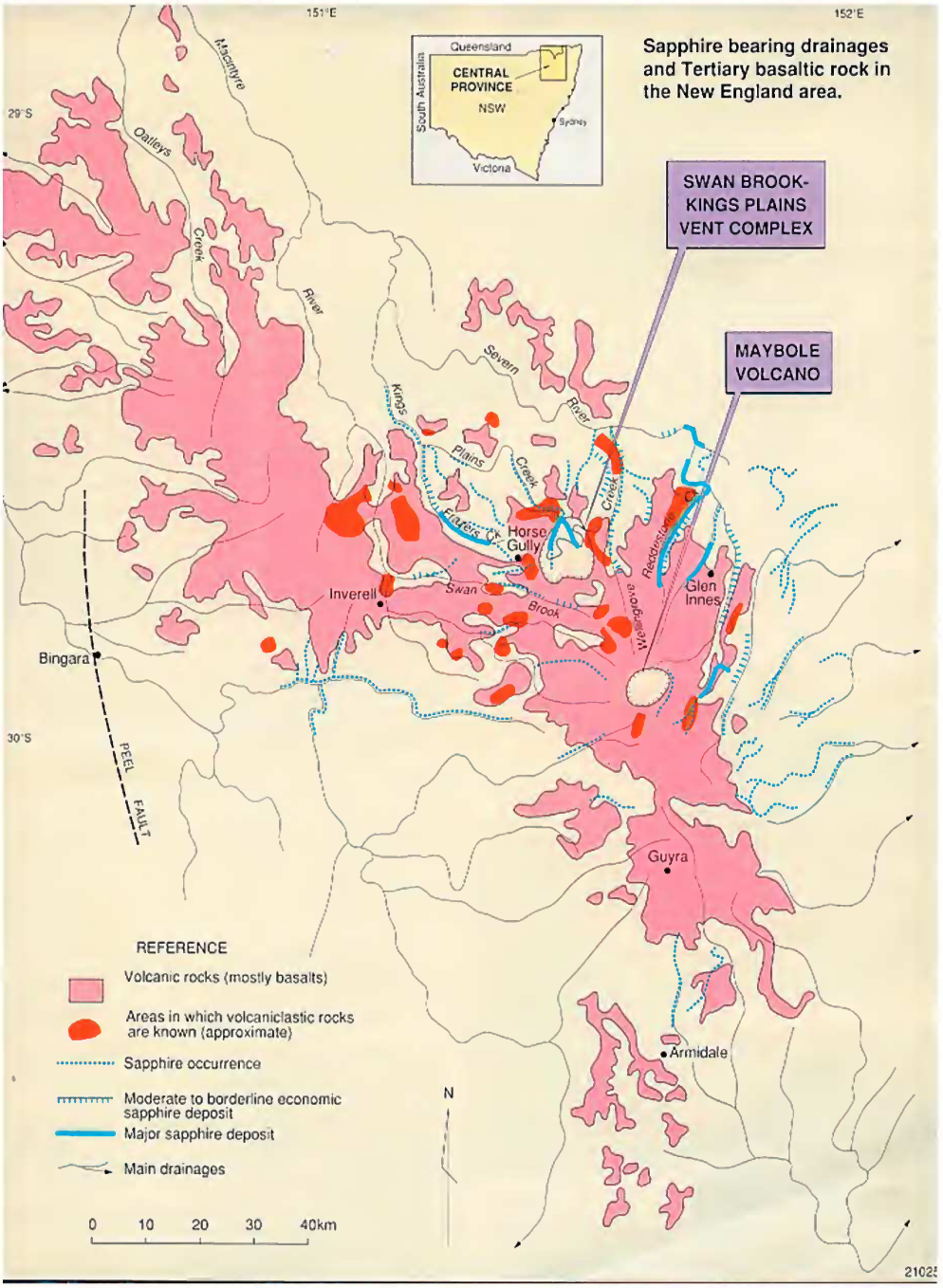

Figure 2. New England, NSW, basalt fields (pink), volcaniclastic deposits (red) and alluvial gem leads (blue). The basalts east of a line through Inverell are mostly alkaline basalts with older ages > 30 Ma, while those to the west include tholeiitic and alkaline basalts mostly with younger ages < 30 Ma. Map courtesy of Gemmological Association of Australia.

Figure 3 (left). A western New England basalt flow capping diamond-bearing alluvial beds. Round Mountain Mine, Copeton area. Photo F. Lin Sutherland.

extensive Mount Russell Volcanics and restricted Dera Dera Volcanics, and two small regions of silica-undersaturated basalts, the Inverell Volcanics and Bingara Volcanics (Vickery et al. 2007). Previous dating results were largely K-Ar ages. McDougall and Wilkinson (1967) cited a range of 20.9 ±2 to 18.5 ± 2 Ma for the tholeiitic Mount Russell – Inverell basanite sequence, while Vickery et al. (2007) reported 23.9 ± 0.3 Ma for a Derra Derra basanite and 22.6 ± 0.5 Ma for a Bingara hawaiite. An Inverell basanite, re-examined by Cohen (2007), gave a more precise

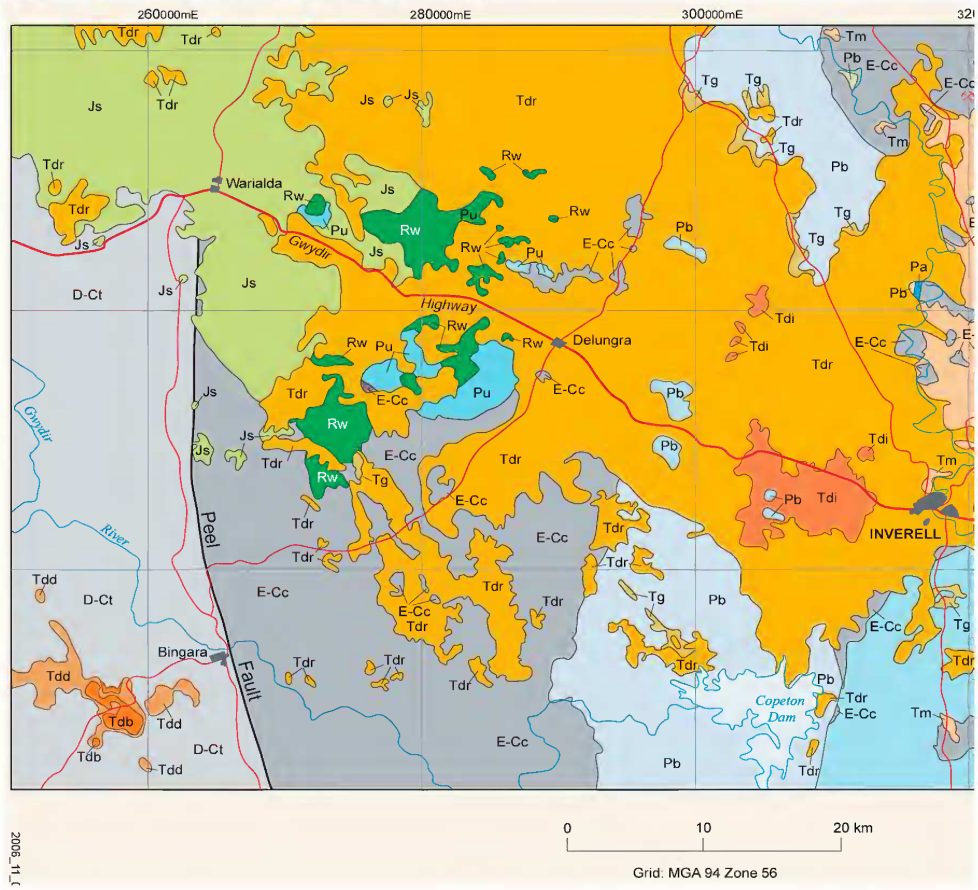

Figure 4. Portion of Inverell 1:250 000 Geological Map Sheet (Vickery et al. 2007), showing details of the Delungra Volcanic Suite basalts (Tdr Russell Volcanics, Tdi Inverell Volcanics, Tdd Derra Derra Volcanics,Tdb Bingera Volcanics) and underlying geological units (Tg Cenozoic gravels, Tm Maybole Volcanic Suite, Js Surat Basin, Rw Warialda Trough, Pu Uralla Supersuite, Pb Bundarra Supersuite, E-Cc Central Block, D-ct (Tamworth Belt), with red lines (roads), blue lines (rivers and dams). Other rock units east of Inverell are not designated. The three latitudinal grid lines lie at 6740000nN, 6720000mN and 6700000mN in descending order.

^{40}Ar-^{39}Ar age of 21.3 ± 0.4 Ma. These results suggest Delungra volcanism was active from ~ 24 to 21 Ma.

The extensive Mount Russell Volcanics in microscope sections exhibit sub-ophitic intergrowth of clinoproxene and plagioclase within a crystallisation sequence of olivine-plagioclase-clinopyroxene-magnetite (Vickery et al. 2007). Chemically, the rocks are quartz tholeiites, with normative quartz ~ 1 –25 %, hypersthene 44–63 % and diopside 33–37 %. They have relatively high SiO_2, Al_2O_3, and Zr/Nb and low TiO_2, MgO, Zr , La/Yb_N and Dy/Yb_N in comparison to the more undersaturated Inverell and Bingara basalts. The smaller Derra Derra Volcanics field shows similar tholeiitic petrology to the Mount Russell field, although slightly lower in SiO_2 and higher in Al_2O_3, while some transitional basalts lack normative qz. Trace element profiles are less elevated than in Mount Russell suites, apart from a distinct high Rb content, while REE profiles show slight enrichment.

The restricted low-silica Bingara and Inverell Volcanic Fields contrast markedly in their petrology from the tholeiitic fields. They are richer in olivine, typically in embayed phenocrysts and microcrysts, and contain feldspathoidal minerals in the groundmass. Analcime in Bingara Volcanics hawaiites can form up to 40 % of the rocks. In Inverell Volcanics basanites, nepheline with associated analcime, cancrinite, zeolites and alkali feldspar can form some 50 % of the rock. The accessory Fe-Ti oxide mineral in these Si-difficient rocks is largely ilmenite rather than the magnetite-ulvospinl series found in the tholeiitic suites.

Trace element and isotope results on the Delungra Volcanic Suite provide insights into the genesis of its basalt fields (Vickery et al. 2007). Normalised REE ratios suggest that the low-Si Bingara and Inverell basalts with the highest Dy/Yb_N (2.5 – 3.2) and La/Yb_N (34 – 57) values represent small volume partial mantle melts from deeper garnet-bearing peridotitic mantle. In contrast lower Yb_N (1.4 – 2.5) and La/Yb_N (4 – 6) values in the Mount Russell Si-rich basalts indicate larger volumes of partial mantle melting of spinel- bearing peridotite mantle, with other trace elements suggesting incorporation of crustal materials. Measurements of isotope ratios of $^{87}Sr/^{86}Sr$ and $^{143}Nd/^{144}Nd$ in the rocks showed that the Bingara and Inverell basalt $^{87}Sr/^{86}Sr$ (~ 0.7040 – 0.7043) and $^{143}Nd/^{144}Nd$ (0.5127) fall within the main field for East Australian central volcano plume signatures. The Mount Russell basalt values ($^{87}Sr/^{86}Sr$ 0.7048; $^{143}Nd/^{144}Nd$ 0.5127) lie slightly outside the plume signature field, but along the same trend line for the Bingara-Inverell basalts. The data suggest all these fields are derived from a similar plume source, although Mount Russell basalts show crustal contamination effects.

Nandewar Central Volcano

The Nandewar volcano has a NNW – SSE trend, probably partly controlled by faulting in the Devonian-Carboniferous basement (Dawson et al. 2003; Cohen 2007; Fig. 5). Considerable erosion of the original structure has revealed much of its basaltic and felsic extrusions and feeders (Figs 5 – 9). Alkali rhyolite flows occupy much of the central region and include an alkali monzonite intrusion, while the northern shield exposes plugs and domes of comenditic rhyolite. Evolved flows in the southern flank are punctuated by a cluster of plugs and flows of alkali trachyte, which includes the high point of Mount Kapatur. A surface reconstruction of the original volcano (Sutherland 1995), depicted two main craters remaining at the north and south ends. These would mark eruptive vents above the two plug and dome sites.

The most accurate dating of the volcanic sequence within the Nandewar volcano and its felsic centres rests on four ^{40}Ar-^{39}Ar ages determined by Cohen (2007), given in a summary plot of the volcano's migratory relationships with the leucititic migratory line to the west (Cohen et al. 2008). A high level basalt, three trachytes and a rhyolite gave a restricted age range of 18.9 – 18.5 ± 0.2 Ma (Figure 5).This restricts activity compared with the K-Ar age range of 21.1 ± 1.5 – 17.4 ± 0.8 Ma (Cohen 2007). The only mafic $^{40}Ar/^{39}Ar$ age lies in the upper volcanic levels, which probably confines basal basalt eruptions to within 21– 18.7 Ma.

Several studies describe Nandewar mineralogy, petrology and genesis of the alkaline rock suites. Abbott (1969) listed an evolution from rare olivine basalt through intermediate rocks such as hawaiites, mugearites and benmorites into silicic end member rhyolites. Low oxygen fugacities in the magmas controlled the compositions of crystallising mafic minerals. Pyroxenes included Ca-rich augite, Na-rich hedenbergite and hedenbergite, while more evolved rocks crystallised sodic amphiboles of the riebeckite – arfvedsonite series Feldspar ranged from calcic-plagioclase into anorthoclase and alkali feldspars in compositions near Ab_{65} Or_{35}. Extreme crystal fractionation processes were invoked for producing the observed rock compositions.

The role of fractional crystallisation in the magmas to produce the assemblages was further investigated by Stolz (1985). He studied slightly saturated hawaiite through trachyandesite and tristanite into comendite. Tristanite is a type of K-

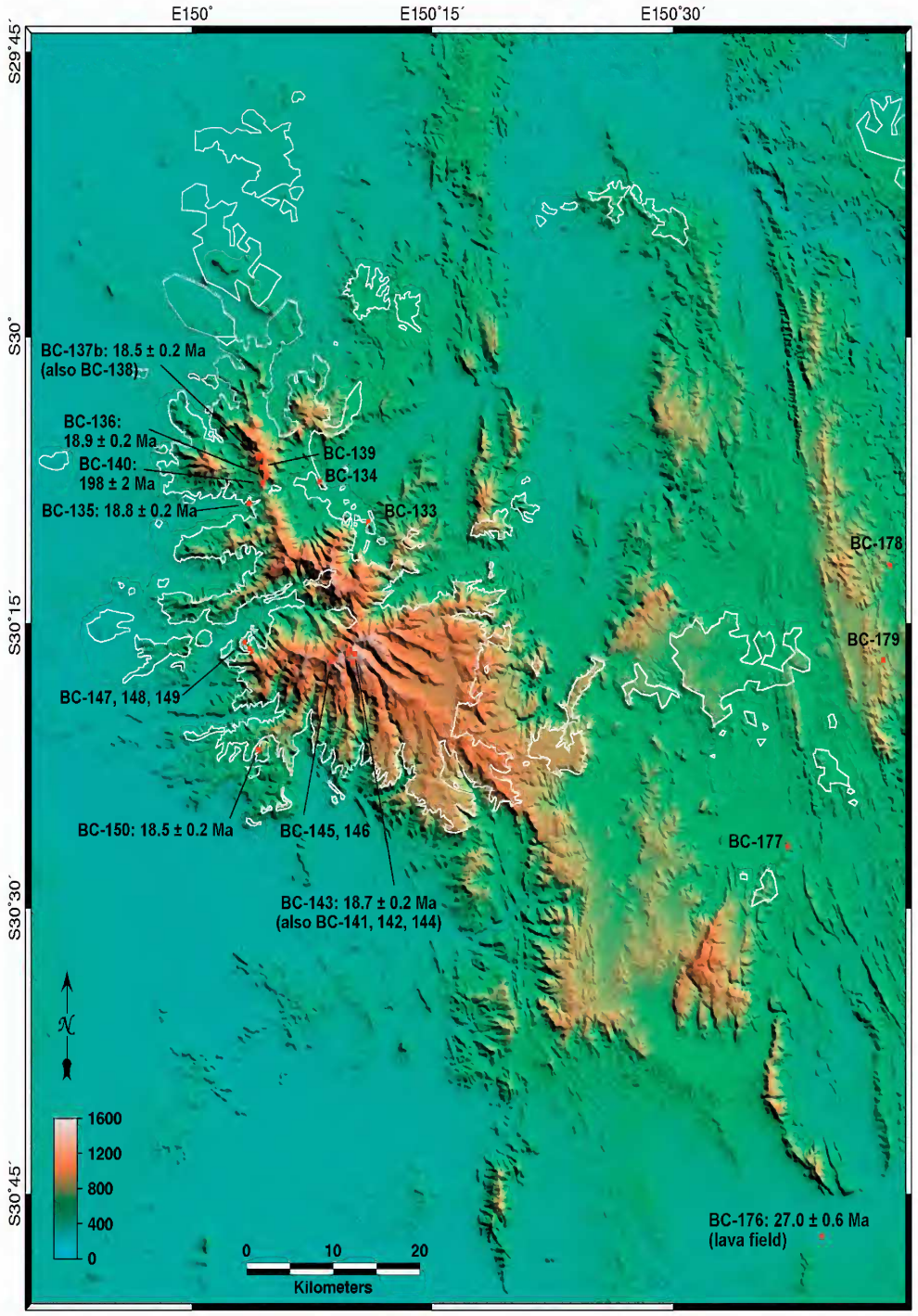

Figure 5. Nandewar Volcano, showing topographic relief based on Digital elevation modelling (DEM), used for locating sites of Ar – Ar ages (Ma), image Cohen (2007).

Figure 6. View of northern profile of Nandewar Volcano, looking north westerly from Killarney Gap, Bingara- Narrabri Road, towards Castle Top Mountain a flow remnant with a dyke outcrop on its eastern side. Photo Ben Cohen.

Figure 7. Sawn Rocks, showing an alkali rhyolite exposure, with well-developed cooling columns, Killarney Gap, S side Bingara- Narrabri Road. Photo Ben Cohen.

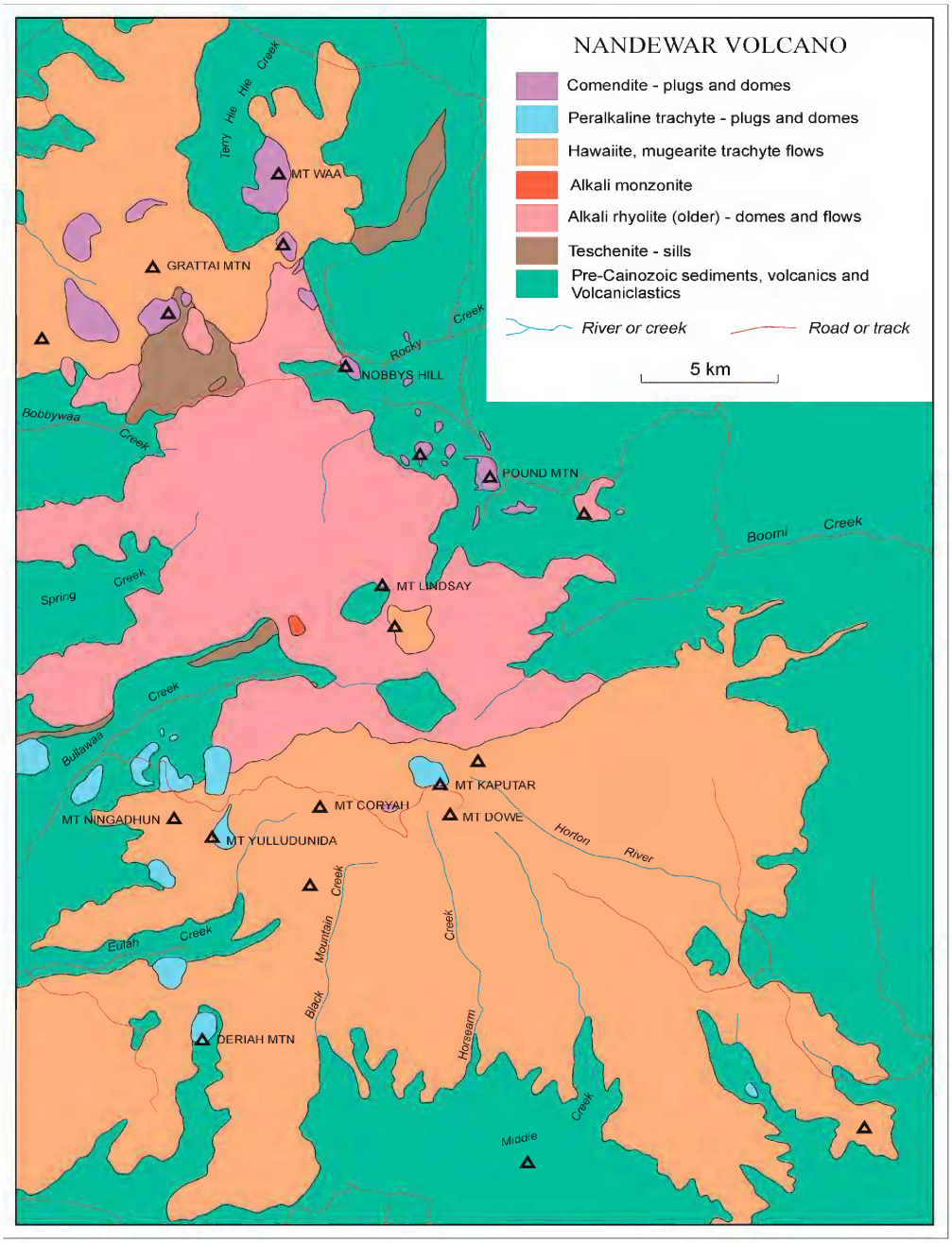

Figure 8. Nandewar Volcano, simplified geological map, with legend. Image Morris Duggan.

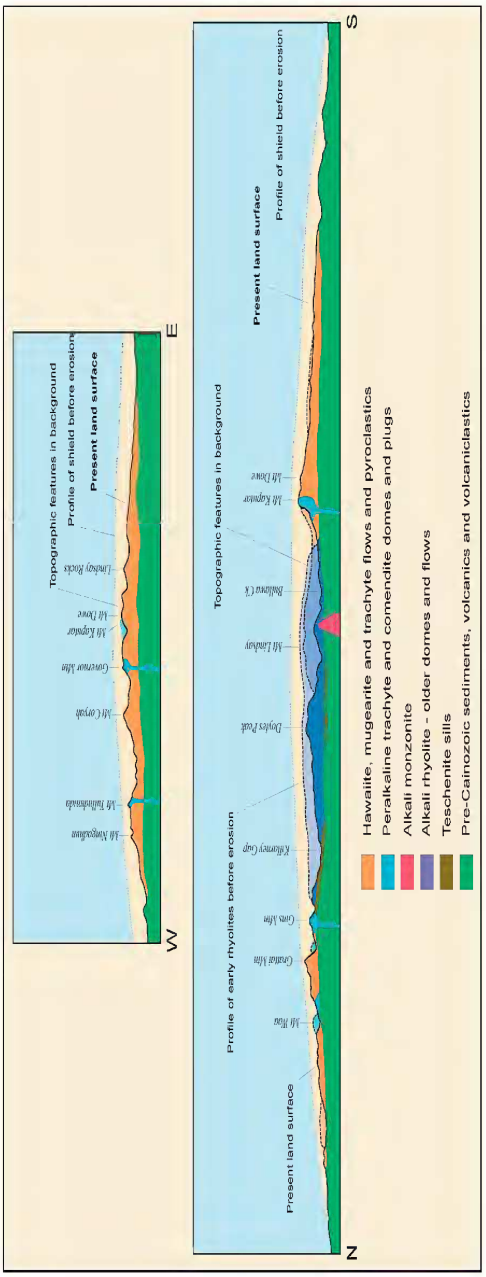

Figure 9. Nandewar Volcano, N-S and W-E profiles, present and past. Image Morris Duggan.

rich trachyte between trachyandesite and trachyte in composition, typical in silica-saturated alkali suites often associated with hot spot-related provinces (Whitaker et al. 2007). At Nandewar, parental magmas were regarded as partial melts of mantle peridotites containing varying amounts of accessory amphibole, mica and apatite. The range of trachytes and rhyolites, however, was difficult to replicate from the mineralogy in the less fractionated rocks. An alternative model was proposed where changes in the melt chemistry took place in the liquid state. Late-stage additions and loses of volatile components were considered as significant modifiers in abundances of alkali elements and trace element contents in magmas during volcanic growth.

Mineral compositions in the volcanic suites were closely studied by Stolz (1986), in relation to magmatic genesis. Olivines, calcic pyroxenes and amphiboles in suites evolving from hawaiite, through trachyandesite to comendite show marked decreases in Mg values (100 Mg / Mg+Fe) within the sequence. Sub-calcic clinopyroxenes and Al-enriched orthopyroxenes indicated crystallisation of hawaiites at pressures between 0.6 – 0.8 GPa. Some trachyandesites contain crystals of plagioclase and Ti-bearing magnetite that suggest crystallisation as cumulates at moderate pressures. Evolution of comendites took place at lower pressures. The Fe-Ti oxide minerals in trachyandesites and comendites indicate trends of cooling temperatures and a decreasing oxygen activity in the crystallising magmas. Some Ti-bearing magnetite and ilmenite developed rims of aenigmatite, in more alkaline-rich rhyolites, suggesting periodic cessation of the oxide crystallisation. Rhyolites in the lower central part of the volcano, however, contain Fe-Ti oxides formed under more highly oxidising conditions.

A summary on Nandewar Volcano petrology included details of field outcrops and settings (Duggan et al. 1993). The volcanic suite was subsequently investigated using a petrogenetic experimental simulation of the Nandewar rocks (Nekvasil et al. 2004). Rock powders were run at various pressure and temperature (PT) conditions under different bulk water contents. Nandewar compositions could arise from a hy-normative hawaiite starting point and fractionate it into sodic rhyolite at P (0.93 GPa), T (1200 – 1100° C), bulk water content at ~ 0.5 wt% and low oxygen activity below the fayalite-magnetite-quartz buffer. The mildly alkaline hawaiite, matching a partial mantle melt at ~ 60 km depth, became increasingly alkaline through strong early clinopyroxene crystal fractionation, with suppression of the feldspar crystallisation. Dominant crystallisation of Ti-rich amphibole, kaersutite, at

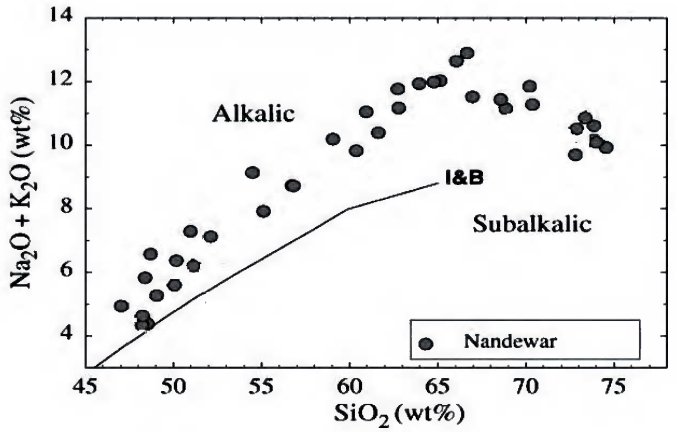

Figure 10. Total Alkalis (Na2O + K2O) –SiO2 diagram showing plots of Nandewar suite analyses from Abbott (1969) and Stolz (1985). Note trend of increasing Alkali content with turn around and slight decline at higher silica levels typical of many hot spot related suites. Diagram modified from Nekvasil et al. (2004). Dividing line I & B between alkalic and subalkalic fields is from Irvine and Baragar (1971)

mid-crustal PT in the middle stages (~ 30 km in depth and ~1100 – 1050° C), pushed compositions towards rhyolitic melts. The changes were pressure sensitive and at mid-crustal values generated K-enrichments in melts. Evidence for multi-stage ponding and crystallisation stages within the melts themselves helps to explain the difficulties Stolz (1985) had in calculating matching assemblages. Nandewar alkali enrichment with SiO_2 (Fig. 10) and other oxide trends (not shown) matches patterns found in alkali shield volcanoes elsewhere, as in the Azores, Atlantic, Clarion Island, Mexico, and Ascension Island, Southern Ocean (Nekvasil et al. 2004).

The full story of Nandewar Volcano activity awaits further resolution. A mantle-derived nephelinite sill with ultramafic inclusions and high pressure megacrysts intrudes the Permian sequence below its northeast side (Wilkinson 1975). Such rocks appear in the nearby plume-related late nephelinites in the Inverell Volcanics, west New England. The Nandewar nephelinite may mark early low-volume deep melting as the area encroached over the hotspot plume, or even late activity as it passed beyond plume influence. The nephelinite's actual relationship to Nandewar Volcano activity, will need precise dating.

Warrumbungle Central Volcano

This is the best age-controlled central volcano in the NW New South Wales chain, where results have clarified many relationships between various landmark volcanic exposures within its landscape features (Figs 11, 12). The volcanic features (Fig.

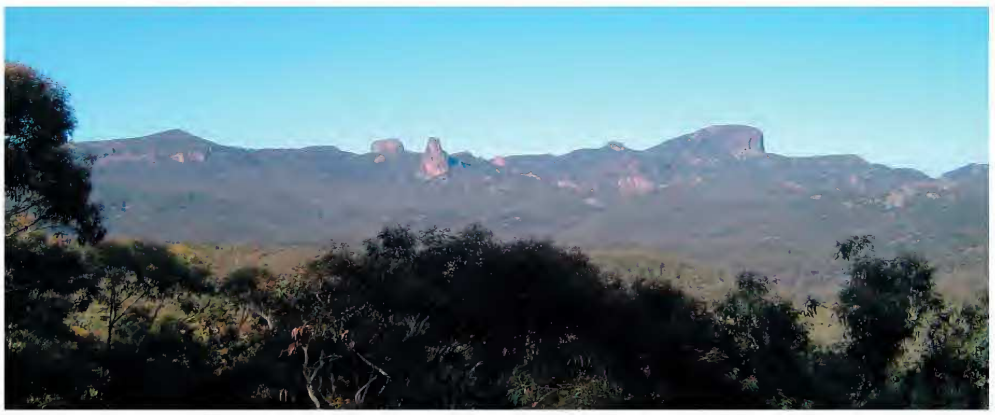

Figure 11. Warrumbungle Volcano, view of Grand High Tops circuit, looking southward, showing intrusive features in the central region. Prominent features include Needle Mountain, extreme left, Crater Bluff (far left), Belougery Spire (left), The Breadknife (left centre), Bluff Pyramid (right) and Bluff Mountain (far right). The Breadknife and Bluff Mountain have Ar –Ar age dates, at 15.2 ± 0.3 and 15.5 ± 0.2 Ma. Photo Ben Cohen.

Figure 12. Crater Bluff (foreground), looking south to Tonduron Spire. Photo Ben Cohen.

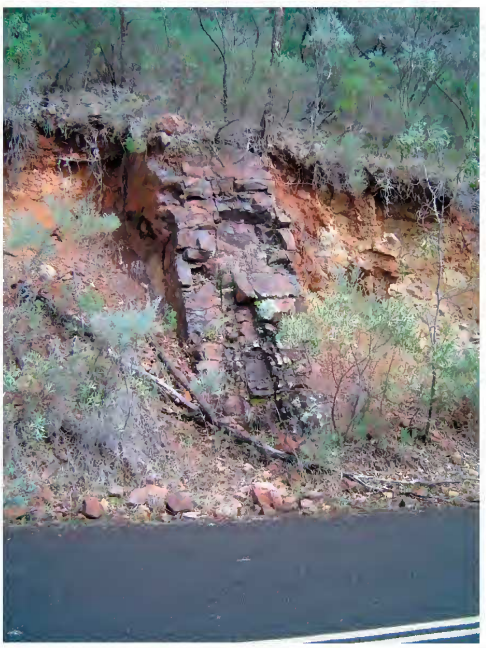

13) largely intrude and/or overlie the Jurassic basin cover (Dugan and Knutson 1993; Dugan et al. 1993; Dawson et al. 2003). A cross section of the volcano with suggested structure and possible original profile is presented in Fig. 14. Sixteen K-Ar ages ranged between ~17 – 13 Ma for the sequence. The $^{40}Ar/^{39}Ar$ dating at 9 sites (Fig. 15) constrained the age range to 18.0 ± 0.2 – 15.2 ± 0.2 Ma (Cohen 2007). Cohen confirmed the activity spanned a magnetic polarity reversal switch from normal, through transitional to reversed magnetism. He also suggested some domal features (Duggan and Knutson 1993; Duggan et al.1993) were probably plugs. Further $^{40}Ar/^{39}Ar$ dating by Crossingham et al. (2018) on trachybasalt and trachyandesite rocks gave ages from 17.8 ± 0.1 to 16.8 ± 0.1 Ma. These ages lie within the overall $^{40}Ar/^{39}Ar$ range for Warrumbungle Volcano, but preceded the recorded late silicic activity between 16.3 ± 0.1 and 15.2 ± 0.3 Ma (Cohen 2007).

Figure 13 (Left). Trachyte dyke intruding pyroclastic beds, lower section Mount Woorut sequence, Siding Springs Road, 0.7 km NE of John Renshaw Drive junction. Photo Ben Cohen.

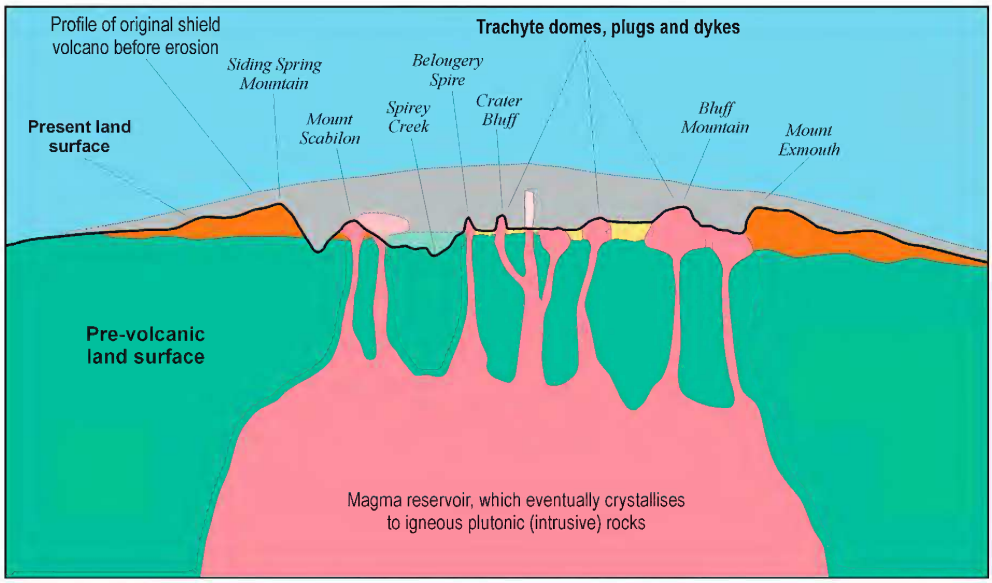

Figure 14. Warrumbungle Volcano, showing simplified geological section interpretation of present structure and original surface profile. Image from Duggan and Knutson (1993). This section pre-dates recent re-mapping of the volcano geology and possible modifications in its interpretation (Bull and Troedson, 2018; Troedson and Bull, 2018).

A comprehensive survey of Warrumbungle Volcano petrology (Duggan et al. 1993), indicated a strongly bimodal distribution with peaks in the hawaiite-mugearite and trachytic ranges. The more mafic rocks dominated in the outer north and south flanks and contain forsterite, Mg-rich olivine, as an early crystallisation mineral. A few hawaiites contain ultramafic inclusions, mostly pyroxenites and megacrysts of Al-bearing and Fe-rich augitic clinopyroxene. Less evolved alkali basalt and more evolved benmoreite are rare types among the mafic series. Trachytes dominate the central part of the volcano, where flows up to 50 m thick form the main shield lavas, and also compose small lava domes elsewhere. Plugs, dykes and domes of such rocks are prominent in the central vent area, such as around the Grand High Tops circuit (Fig. 11), but also form isolated peaks in the east and south flanks.

The trachyte suite typically contains Fe-rich olivine, the mineral fayalite, and includes both alkali and meta-aluminous compositional types. The Warrumbungle petrological evolution was considered to mostly represent compositional magma fluctuations across a critical thermal divide that directed crystallisation into silica-saturated and silica-under saturated feldspathoidal-crystallising paths. Peralkaline felsic magmas dominated the abundant explosive pyroclastic deposits through the sequence. Overall, these magmas typically crystallised sodic clinopyroxene, minerals in the hedenbergite-acmite series, which may contain abnormally high values of Zr (Duggan 1988). The sodic amphibole arfvedsonite is also common in the peralkaline rocks. In addition, the sodium, titanium, iron silicate mineral, aenigmatite, is present in many trachytes. Some exceptionally Ti-poor, silica-undersaturated trachytes contain wilkinsonite $Na_2 Fe^{2+}_4 Fe^{3+}_2 Si_6 O_{20}$ (Fig. 16). This is a new member of the aenigmatite group first described from Mount Bingie Grumble in the Warrumbungles by Duggan (1990). It was named after an Australian petrologist, the late Professor John Wilkinson from the University of New England, Armidale, NSW, for his seminal studies on the nature and evolution of alkaline rocks, especially in eastern Australia.

Detailed geochemical analyses on two Warrumbungle peralkaline trachytes were compared with Nandewar, Canobolas and other such East Australian Mesozoic-Cenozoic examples (Ewart et al. 1985; Ewart 1985). The O isotope values for feldspars in Warrumbungle trachytes were noticeably higher than in a Nandewar, Mount Kapatur rock. Subsequent detailed petrological studies on

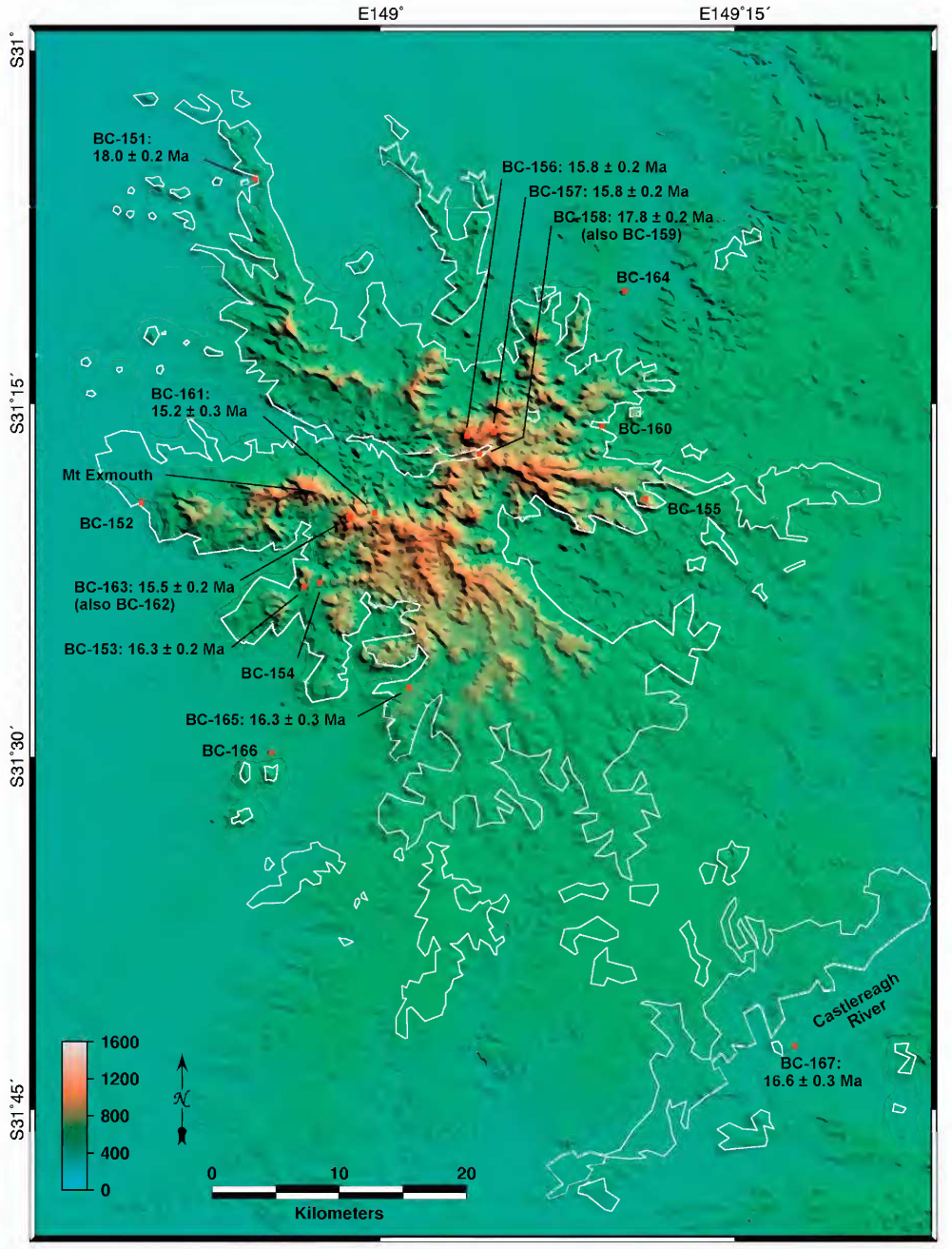

Figure 15. Warrumbungle Volcano, showing topographic relief based on DEM modelling, with sites used in Ar –Ar age dating (Ma). Image Ben Cohen.

Figure 16. Photomicrograph of wilkinsonite-bearing trachyte in thin section. The large white crystals are phenocrysts of anorthoclase feldspar and the dark crystals in the groundmass include both the sodic pyroxene aegirine and the new mineral species wilkinsonite. Field of view is 100 mm in width. Photo Morris Duggan.

Warrumbungle Volcano included close attention to its phonolitic and trachytic suites (Ghorbani 1999; 2003). Warrumbungle Volcano is the most investigated central volcano in the NW New South Wales migratory chain. The pyroxenes were used by Ghorbani and Middlemost (2000) to unravel the complex magmatic petrogenesis, which identified a high pressure, depleted mantle peridotite source and Al- and Fe-enriched crustal magma chambers. One nepheline-normative mafic rock included omphacitic pyroxene with very high K contents (up to 2.3 wt %), which suggested a deep mantle source.

Mafic to intermediate petrology in the Warrumbungle sequence was targeted recently by Crossingham et al. (2018). They examined crystallisation processes in the feeder systems below the volcano. The hawaiite and mugearite lavas ranged from aphanitic to glomeroporphritic in texture. The macrocrysts in the rocks included both antecrysts that represent earlier crystallisations in the volcano, brought up and recycled into the later magma, and phenocrysts that grew within the erupting magma. Macrocrystic minerals were commonly plagioclase, and clinopyroxene, which included pink Ti-rich augite and lower Ti- and Mg- content green augite. Olivine macrocrysts are rare, except in one lava in which crystal cores are Mg-rich, although some are zoned to Fe-rich rims. Clinopyroxene macrocrysts range from pinkish Ti-rich augite to greenish augite with lower Mg and Ti contents and commonly show spongey textures. Magnetite macrocryts are usually present.

In synthesising their data, Crossingham et al. (2018) concluded that Warrumbungle Volcano grew in three stages. Initial-stage magmas fractionated olivine and some clinopyoxene and evolved during ascent. Second stage crystallisation became more complex. Magmas divided into separate batches of different ages and compositions and sampled materials from crystal mushes formed in melts at depths of ~ 40 km. This led to a final stage of magma mingling and increased mixing of antecrysts and phenocrysts in ascending recharges of magma at higher levels. The Mg content in the studied lavas differed during the stages of growth and fractional crystallisation of mineral phases. First stage growth lavas showed the highest MgO range (~ 3.5 – 7.5wt %), second stage lavas the widest MgO range (~ 0.5 – 7.5 wt %) and the final stage had a slightly restricted range (~ 2 – 5 wt %). These growth stages, their timing and various depths of magma generation and recharging, and their associated mineral crystallisations are summarised in Fig.17 (after Crossingham et al. 2018). This Figure also shows differences in growth and crystallisation in Warrumbungle Volcano and its migratory twin, Comboyne Volcano, east of the Dividing Range.

The geological story of Warrumbungle Volcano is far from finished. Exposures found after the ravages of fire and flood in 2013, allowed more detailed mapping of their features and are listed in the 2018 Symposium abstracts. They include stratigraphic refinements (Troedson and Bull, 2018), detailed studies on pyroclastic deposits and evaluation of late radial trachytic dykes in the magmatic and inflation uplift history (Bull and Troedson 2018), geophysical observations of signature responses from airborne and satellite surveying (Carlton and Bull 2018), erosional expressions in alluvial depositions and mass waste movements (Thompson 2018; Tulau et al. 2018) and descriptions of embedded fossiliferous horizons (Holmes 2018). An informed stage now exists for other flora, fauna, environmental, educational and recreation projects within the time-honoured volcanic edifice.

Canobolas Central Volcano

The smallest and youngest central volcano in the NW New South Wales chain, Canobolas, retains a subdued summit core rising above its remanent basaltic shield outflows (Cohen 2007; Figs 18, 19). Initial K-Ar dating gave 13.0 ± 2 – 11.2 ± 0.3 Ma, while 5 Ar–Ar ages gave a similar range 13.2 ± 0.3 – 11.2 ± 0.3 Ma (Cohen 2007). Mafic samples gave both early (13.2 Ma) and late (11.6 Ma) ages, while

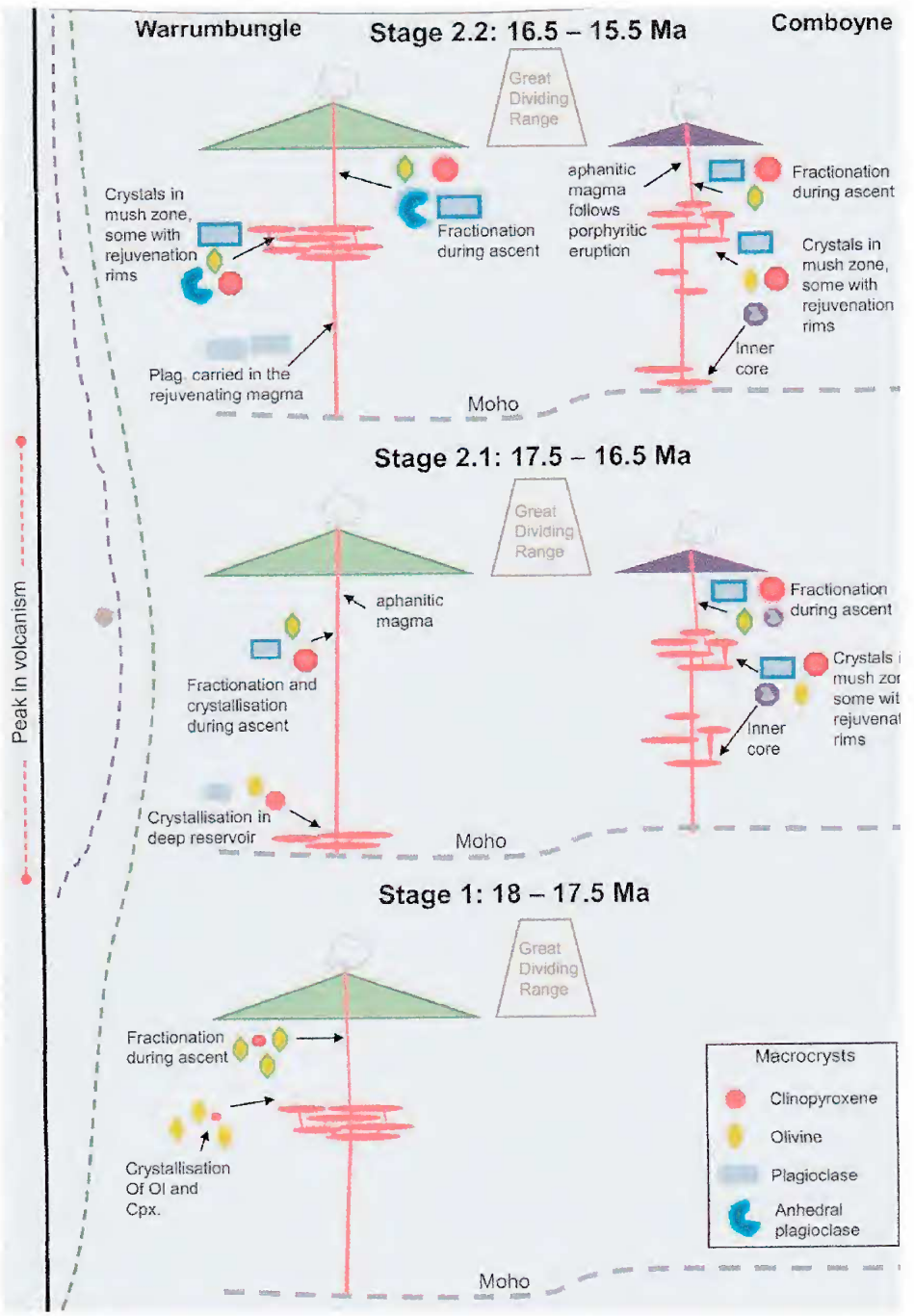

Figure 17. Magmatic and eruptive growth history of Warrumbungle Volcano, compared with the co-eval Comboyne migratory volcano, east of Dividing Range (Crossingham et al. 2018).

Figure 18.Canobolas Volcano in profile, showing summit region (centre distance) rising above flanking outcrops of eroded flows of its former basaltic shield. Photo Ben Cohen.

felsic ages (11.9 – 11.6 Ma) suggest overlap with the mafic eruptive range, as supported by field data (Middlemost 1981; Cohen 2007).

Previous petrological studies on the volcano were summarised by Middlemost (1981). His studies revealed a complete series of evolved members from hawaiite to rhyolite. Initial eruptions of mafic shield lavas preceded growth of a central complex as more evolved melts became admixed with further mafic events. The early mafic flows and pyroclastic deposits were mostly hawaiite and flow sheets up to 150 m thick built voluminous south easterly sequences. Mafic flows descending north western volcanic flanks flowed into a SE tributary drainage of the Lachlan River. Flows descending northern flanks travelled up to 70 km from the vent region into tributary drainages flowing north into the ancestral Macquarie drainage (Cameron et al. 1999; Tompkins and Hesse 2004). The Canobolas central summit growth included emplacements of felsic domes, dykes, plugs, flows, pyroclastic and volcanoclastic deposits (Figs 20 – 22).

Middlemost (1981) depicted the fractionation sequence using plots of MgO + CaO against Na_2O + K_2O. Representative proportions of analysed rock types (given here as %), included hawaiite (25%), mugearite (6%), bemoreite (8%), trachyte (47%) and rhyolite (14%). A trend of decreasing (MgO + CaO) from hawaiite to trachyte levelled out at low values and then trended into the rhyolite field. This trend mirrored the Total alkalis vs Silica diagram trend for Canobolas and also Nandewar evolution (Figure 10), but instead uses a mafic component rather than silica. At Canobolas voluminous trachyte generation dominated the central summit growth. A massive trachyte flow remnant 8 km long, 3 km wide and 30 m thick descended the southern extremities of the central vent apron (Panuara flow). Less voluminous silicic end member rhyolites, mostly comendites, formed an annular domal ring around the central trachytic plug complex. Middlemost suggested the silicic melts were derived by filter pressing and/or volatile release processes within underlying pools of trachytic magma.

Potential fractionation models were studied to establish Canobolas magmatic lineages (Middlemost 1981). This employed least squares calculation using the main mineral phase compositions in the various rock types. Starting with hawaiite, removal of augite (76 wt %), olivine (13%), magnetite (9%), and ilmenite (2%) produced mugearite. Then crystallising calcic plagioclase (52%), augite (27%), olivine (8%), and magnetite (7%) led to benmoreite. Further extraction of calcic plagioclase (75%), Fe-rich augite (13%), ilmenite (7%), and magnetite (6%) yielded trachyte. Alkali rhyolite could be attained with depletion of sanidine (88%), Fe-rich augite (7%), and magnetite (7%), or by removal of Fe-rich augite (88%) and magnetite (12%).

Further trace element (Pb, Rb, Sr, Sm, Nd) and isotope (Pb, Sr, Nd) data for Canobolas mafic lavas were presented by Ewart et al. (1988), who

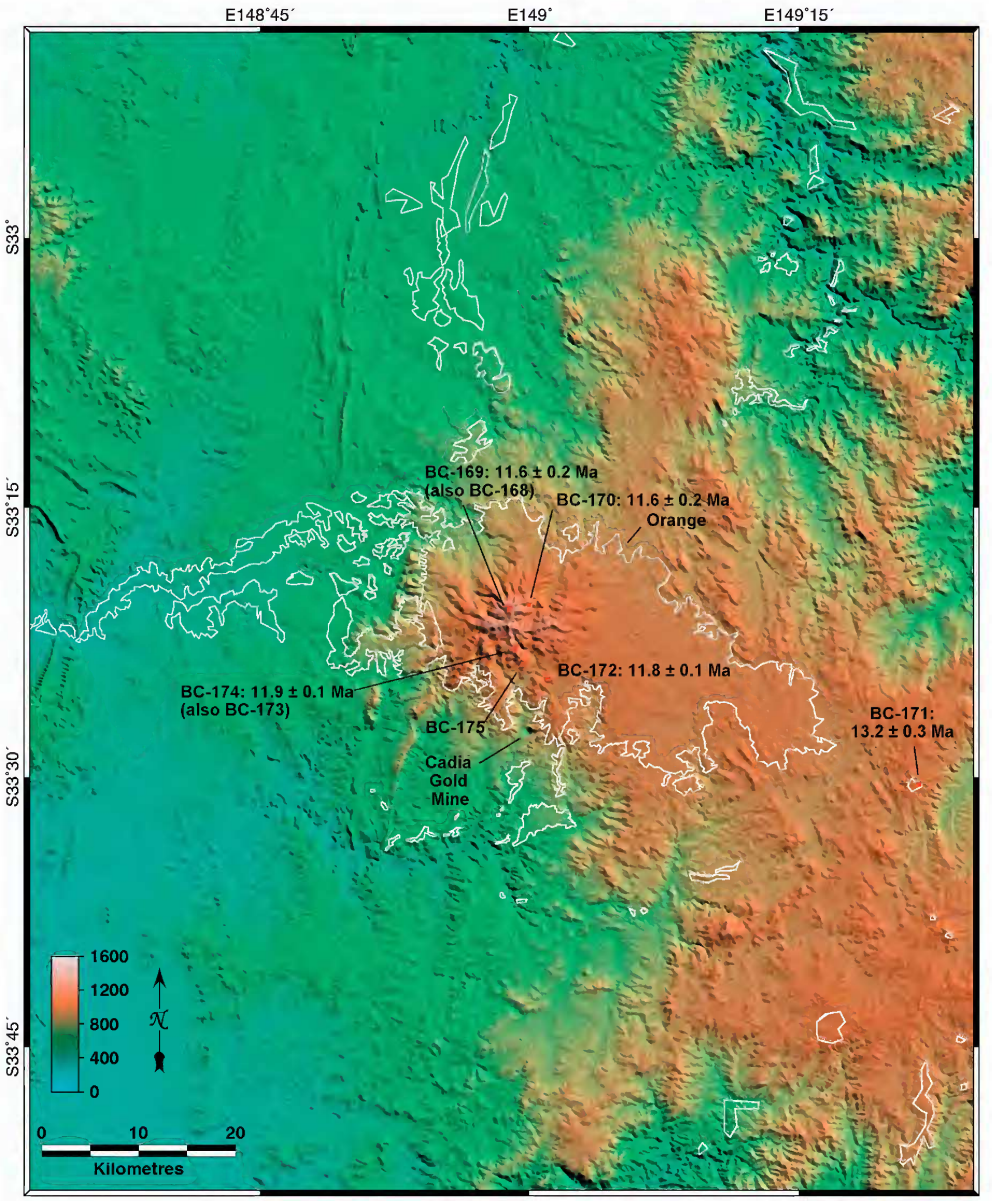

Figure 19. Canobolas Volcano, showing topographic relief based on DEM modelling, with sites used in Ar –Ar age dating (Ma). Image Ben Cohen.

introduced new mafic rock terms, quartz tholeiite and icelandite. End member alkali rhyolites were divided into two types (Pogson and Watkins 1998), a riebeckite-bearing rhyolite found in the larger domes on the volcano and arfvedsonite-bearing rhyolite that formed smaller remnant domes, cones and lavas.

Abecrombie zircon-bearing volcanic outburst

The Abercrombie Province 60 to 100 km SE of Mount Canobolas contains scattered flow remnants and small intrusions of alkali basalts that include

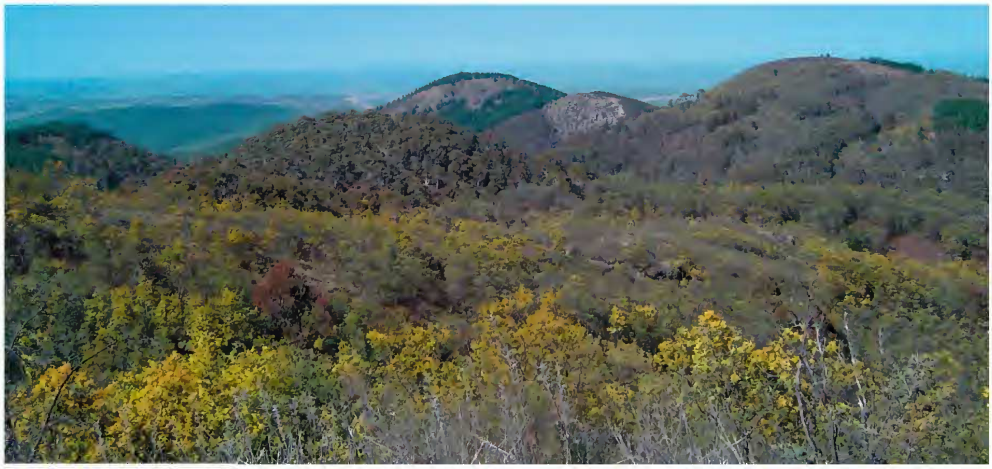

Figure 20. Lava domes of comendite, SE flank of Mount Canobolas. Photo Ben Cohen.

Figure 21. Small dyke, near summit, Mount Canobolas. Photo Ben Cohen.

mantle-derived types (Pogson and Watkins 1998). K-Ar age dating suggested several eruptive episodes between 20 and 16 Ma. A feature of the province is the presence of basalt-derived gem suites within adjacent alluvial deposits. Corroded crystals of gem zircon were dated by fission track counts from radiometric breakdown of U in their structure after thermal resetting during passage in hot magma. The zircons ages record several episodes that correspond with host basalt radiometric age-dates.

Figure 22. Scoriaceous mafic clast with chilled margins, in volcanic breccia, SE flank, Mount Canobolas. Photo Ben Cohen.

Figure 23. Zircon grains polished by magmatic corrosion, largest grain 0.25mm across, retrieved from fluvial sediments, Hopes Creek, Oberon area. Image Ross Pogson, Australian Museum.

One zircon age group stood out, with a young age range that matched the predicted latitudinal position for the East Australian hot spot at that time. The highly polished crystals show magmatic corrosion (Fig. 23), but there is little abrasion. This suggests minimal alluvial reworking of the grains, unlike that found in grains recycled from the older basalt sources. The young zircons were recovered from several sites around Oberon to Kings Plains near Blayney. Fission track ages (6 sites) ranged from 8.6 ± 2.3 to 9.4 ± 2.7 (av. 9.2 ± 2.1) Ma (Sutherland 1993, and Australian Museum Geotrack reports).

Further recent unpublished Ar-Ar dating on Warrumbungle and Canobolas volcanic rocks is available in Jones (2018). These extend the number of dated sites, although the age limits remain within the previous interval given by Cohen (2007).

DISCUSSION

Allied volcanic fields

Miocene volcanic fields in NW New South Wales include a dominant migratory chain of plume-related volcanoes. Three fields evolved into central volcanoes, while a low-volume basalt field to the SE, revealed a young ~ 9 Ma zircon-bearing event that may mark diminished plume activity. Other low-volume basaltic fields lie ~ 100 km SSW of Warrumbungle central volcano near Dubbo. There, they intrude and overlie Triassic-Jurassic Surat Basin beds (Cameron et al. 1999; Dawson et al. 2003). Farther west in NSW, a migratory chain of minor plume-related leucititic volcanoes kept pace with the large Nandewar – Canobolas central volcano migratory chain (Cohen et al. 2008).

The Dubbo basalts have limited K-Ar dating (12.3 – 14.3 Ma), and overlap basalt ages around Gulgong ~ 60 – 80 km east (14.2 –15.2 Ma; Cameron et al. 1999). Such basalt ages at latitudes between the main Warrumbungle and Canobolas central volcano activity prompt possibilities that this flanking basaltic activity may be linked to thermal effects from the nearby plume passage. Petrological study of Dubbo olivine tholeiites showed trace element and isotopic signatures similar to those in eastern Australian central volcanoes (Zhang and O'Reilly 1997). Such plume-related activity may extend back to 20 Ma, based on a K-Ar date on an olivine tholeiite body, 9 km WSW of Dubbo (Sutherland et al. 2012). Evolved K- rich hawaiites in the suite were considered to develop by high pressure fractionation and crustal contamination of the olivine tholeiite magmas. The accompanying basanite and alkali basalts, in contrast, required melting of a deeper source with a composition suggestive of a metasomatised lithospheric mantle.

Miocene leucititic volcanoes form a distinct petrological suite that extends south through outer NW New South Wales (Cundari 1973; Cundari et al. 1978; Johnson 1989). They are part of the longest known migratory continental hot spot chain (Sutherland 1981; Davies et al. 2015). The NSW leucitites formed small volcanic feeders, vents and flows (Figs 24, 25), with Ar-Ar ages between 18–15 Ma (McQueen et al. 2007; Cohen 2008). New high-quality paleomagnetic pole positions were calculated for the leucitites using the Ar-Ar age-dates (Hansma and Tohver 2018). Results confirmed earlier findings and showed the leucitite and Nandewar central volcano paleopole positions were indistinguishable, with a leucitite-related plume positon at 40.3 ± 3.0 ° S.

The mineralogy, petrology and likely genesis of the plume-related leucitites are presented in Johnson (1989). Their plume source differed from the central volcano asthenospheric source and involved lithospheric melting and contamination along a rift line, activated by an underlying plume. Leucititic

Figure 24. Leucitite flow capping, El Capitan, looking from northwest. Photo Ken McQueen.

magma generation was constrained by lithospheric thickness, which exceeded ~ 135 km in depth (Rawlinson et al. 2017a). Unusual baryte-bearing hybrid basalt breccias occur north of Byrock leucitite volcano and included fragments of anorthoclase-nepheline basanite with fractionated pods of baryte-bearing trachyte (Sutherland et al. 2007). These vents may be plume-related, as they lie on the calculated track at ~30° S and show high Ba, a feature found in the leucitites (Davies et al. 2015). Such assignment, however, requires confirmation by dating.

Genesis of the Nandewar-Warrumbungle-Canobolas chain

The rise and fall of these central volcanoes took place within a bending plume trace (Fig. 26). After preliminary lava field activity in western New England, more voluminous magmatism created Nandewar Volcano (600 cubic km), then Warrumbungle Volcano (500 cubic km), before dwindled noticeably in forming Canobolas Volcano (50 cubic km) and finally tailed off into minor lava field activity (volume estimates from Duggan et al. 1993). Nandewar Volcano developed significant rhyolitic inputs, notably alkali rhyolites, whereas rhyolite is scarce in Warrumbungle Volcano and Canobolas only exhibits small rhyolitic events of comenditic type in its summit growth. A study of exposed central volcano feeders in the Glass House Mountains, SE Queensland (Shao and Niu 2015), focused on the genesis of peralkaline and peraluminous rhyolites. They suggested these suites reflected basaltic underplating and crustal contamination effects in their respective magmatic evolutions. Peralkaline trends are well developed in both Nandewar and Warrumbungle volcanoes, particularly in trachytes, which would suggest such underplating took place below those large volume volcanoes. This process also has solid support from earlier studies based on gravity and magnetic data (Wellman 1986; Johnson, 1989).

The West New England – Nandewar – Warrumbungle – Canobolas – Abercrombie trace (Fig.26), is anomalous. It does not correlate with an expected hot spot trace based on Australian plate motion during its eruption period (25 – 10 Ma), nor with the leucitite volcano line to the west or the coastal central volcano and oceanic hotspot chain trends to the east (Sutherland et al. 2012). This can be noted in the Australian and oceanic hot spot traces and plate motion tracks (Fig. 27). Various causes are given to account for bends in Australian central volcano traces, from tectonic shifts caused by former plate collision effects to the north and/or slab break-off effects on the eastern margin (Knesel et al. 2008; Sutherland et al. 2012; Cohen et al. 2013). These events created abrupt changes in the volcanism volumes and migration trends, which are less apparent in the NW New South Wales trace.

Figure 25. Leucitite flow margin, with inward dipping cooling joints, El Capitan. Photo Ken McQueen.

Recent studies show that plume activity can become incorporated into lithospheric edge-driven melting episodes, as in central-western Victoria (Sutherland et al. 2014; Oostingh et al. 2015; Rawlinson et al. 2017a). Studies of lithospheric thickness in eastern Australia above underlying plume sources show its depth can control the volume and nature of the plume-generated mantle melting (Davies et al. 2015). In this study, it is noticeable that the west New England basaltic – triple central volcano – Abercrombie basaltic migration follows the western curved edge of a lithospheric 'cavity' detected under the region (Rawlinson et al. 2017a; cavity C2). Neither the 'cavity' boundary, nor the subsequent volcanic migratory trace match the post- 24 Ma plate motion trend for eastern Australia (Rawlinson et al. 2017b), as shown in Fig. 28. To help explain this anomaly, it is surmised an underlying plume was over-ridden by the 'cavity' margin as plate motion carried the structure across the plume threshold. This diverted the plume and enhanced its activity through lithospheric edge-driven melting along the western 'cavity' margin. Plume activity dwindled and ceased as thicker lithosphere capped its track beyond the 'cavity' structure.

The northwest NSW plume activity was concentrated along the western side of the 'cavity' structure. This may reflect asthenospheric flow motion within the mantle upwelling. In sections modelled through such mantle upwells within the southern 'cavity' structure (C1), which triggered the plume-edge-driven Newer Volcanic basaltic activity, a westerly mantle flow of ~ 2 cm/yr was observed (Rawlinson et al. 2017a). A similar westerly mantle flow component may have directed the plume magmatic interaction towards the western edge of the underlying NW New South Wales lithospheric 'cavity'.

Where did the NW New South Wales central volcano plume originate?

The plume-dominated migratory volcanic trend lines in NW New South Wales all project back into Queensland. There, the central volcano lines extend northward to coastal exposures between Fraser Island and Cape Hillsborough (Sutherland et al 2012; Cohen

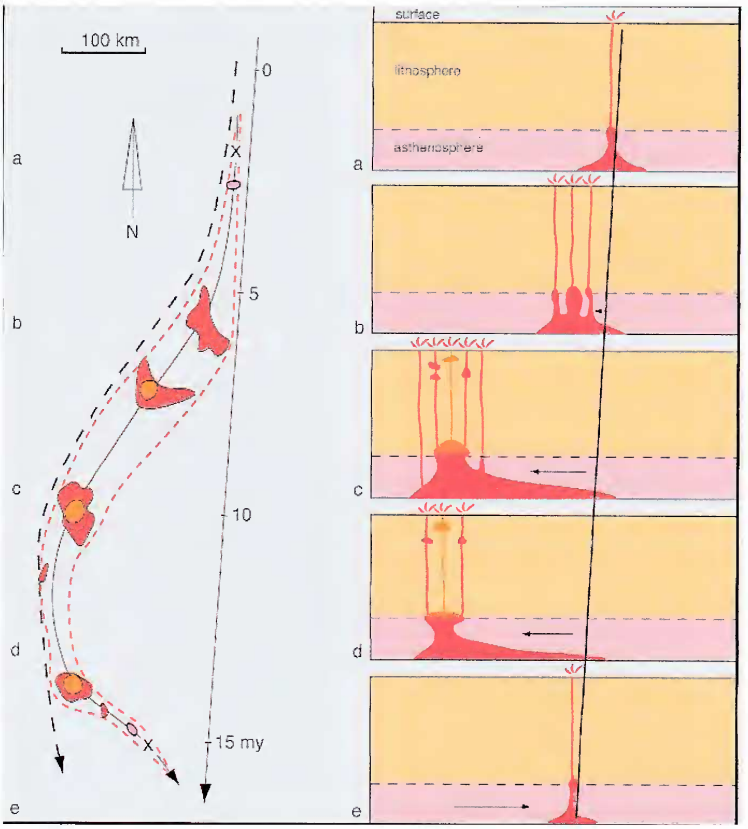

Figure 26. Idealised growth segment for relative New England-Nandewar-Warrumbungle-Canobolas migration. Left panel: Plan of migration growth relative to Australian plate motion trend over 15 Ma of migration, with basaltic areas (red), felsic cores (orange), minor alkaline fields (pink) and zircon megacryst-bearing eruptions (black crosses). Right panel: Lithosphere-asthenosphere cross sections (a – e), showing relative plume and surface volcanism from initiation to cessation (black trend line). Diagram from Sutherland (2003).

et al. 2013). This, central volcano activity is dated back to ~30 – 34 Ma, before its continuity vanishes offshore. Some modelling suggests that these plume trails project back to a major triple point rift-event that formed the Coral Sea – Louisiade – Cato Tough spreading segments (Sutherland et al. 2012). Figure 29 depicts plate motion paths for East Australia, generated from the present dormant locus of the plume system across Bass Strait and western Tasman Sea. The plate migration trends calculated at 10 Ma intervals from the plume locus suggest the NW New South Wales central volcano trends intersects the main thermal spreading arm of the Coral Sea Triple Point between 60 – 70 Ma. Some support for a major Coral Sea thermal event involvement in the past plume activity comes from dating of basalts dredged from the adjacent submerged Louisville Plateau at 55-56 Ma (Kalnins et al. 2015; Richards et al. 2018).

The NW New South Wales central volcano migratory plume track extrapolated northwards intersects the preceding voluminous basaltic-central volcano activity in SE Queensland (Brown et al. 2014). This presents a complicated task in determining its precise path for its earlier plume line connection. A thickened lithospheric spine protrudes eastwards below the connecting NSW border, which would inhibit the intervening plume melting (Davies et al. 2015). A possible link in this low-volume melt zone may be marked by an altered 'leucititic' lava remnant that overlies Mesozoic sandstones near Inglewood, SE Queensland (Wilkinson 1977). This lava, however, lacks precise dating. If plume-related, it would link the NSW trend towards the Main Range Volcano. Here, a small central volcano trace extends northerly from Toowoomba to eastern Bunya Mountain dated at 22–24 Ma (Sutherland et al. 2012). The trace, however, seems too young for migratory connection with Delungra NSW volcanism. A more easterly trend into Fassifern Valley central volcanoes connecting with the 26 Ma Flinders Peak volcano improves timing and links into the coastal SE Queensland plume line (Cohen 2007).

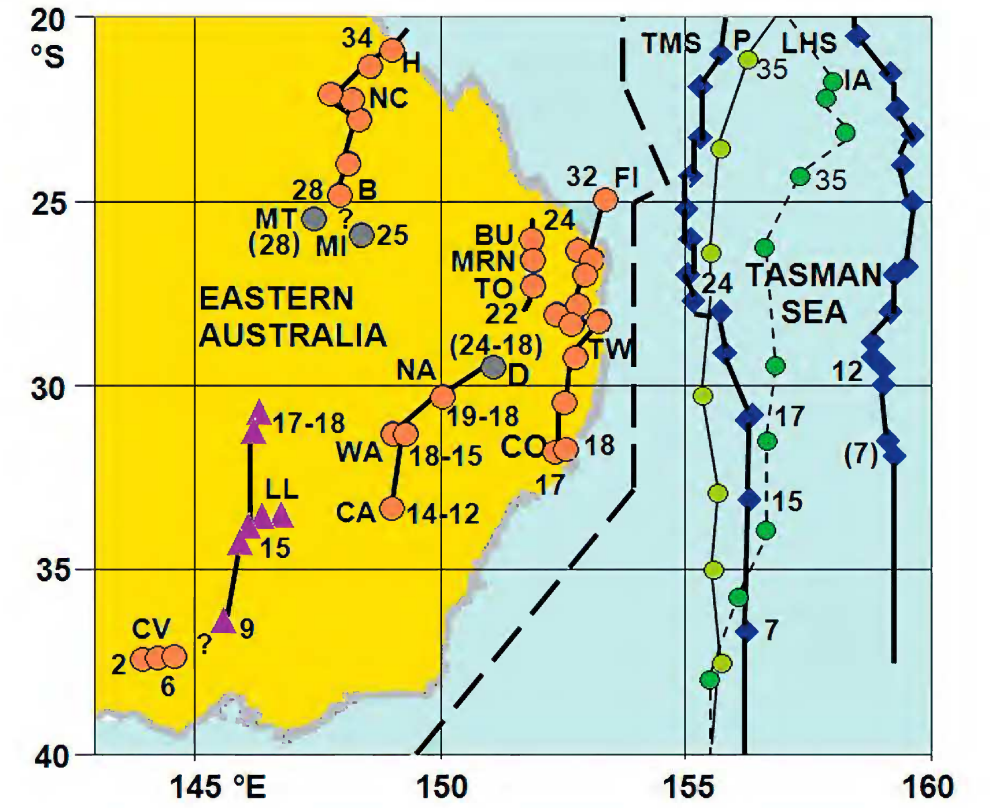

Figure 27. Eastern Australian and oceanic hot spot volcano traces (black connecting lines), with (Ma) and locality codes of central volcanoes (orange red circles), basalt lava fields (purple circles), leucitite volcanoes (purple triangles) and oceanic seamounts (dark blue diamonds). Plate motion tracks at 5 Ma intervals are fixed to Indian Ocean hot spots (thin black line with light green circles) and Pacific Ocean (thin dashed line with dark green circles). After Sutherland et al. (2012), which contains a full volcano code listing. Relevant codes here are D Delungra, NA Nandewar, WA Warrumbungle, CA Canobolas, and LL Leucitite Line.

CONCLUSIONS

The NW New South Wales volcanism is dominantly a mix of 'hotspot' plume-generated basaltic lava fields of both alkali and tholeiitc affinities, central volcanoes with basaltic shields and evolved felsic cores and low-volume leucitic intrusions and flows.

Three significant central volcanoes dominate the main plume-trace, the Nandewar, Warrumbungle and Canobolas Volcanoes, each showing well developed fractionation processes in their evolution, but each showing differences in their petrologic make up.

The plume lines represent surges in volcanic activity between 24 – 10 Ma. Subsequent post-eruptive erosion has exposed spectacular internal volcanic features. The scenic remnants have attracted considerable scientific studies, recreational use and preservation as National Parks and nature reserves.

Volcanoes along the main plume migratory track show an overall rise and fall in eruptive volumes associated with a curving swell and pinch path that does not correspond with the underlying paleo-plate motion of Australia. This suggests an additional eruptive control.

The volcanic rise and fall along the west New England –Abercrombie migration curve follows the western edge of a lithospheric 'cavity' revealed by seismic tomography, suggesting interaction of a plume and lithospheric 'cavity' edge that diverted the plume line.

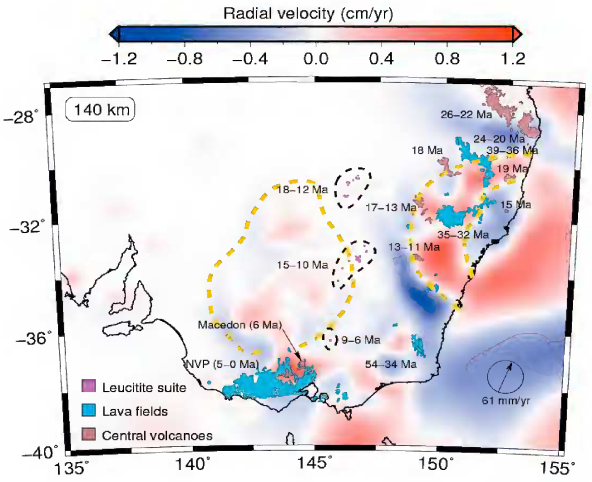

Figure 28. Radial seismic velocity map of East Australian lithosphere at 140 km depth. The eastern coastal lithospheric 'cavity' (152 – 153o E; 29.5o – 35.5 o S) enclosed by a pair of yellow dashed curved lines enclosing faster radial velocities (0.0 – + 1.0 cm/yr). Note its western boundary forms the locus for the NW New South Wales migratory basaltic and central volcano rise and fall between 24 – 11 Ma. Diagram after Rawlinson et al. (2017b; Fig. S8).

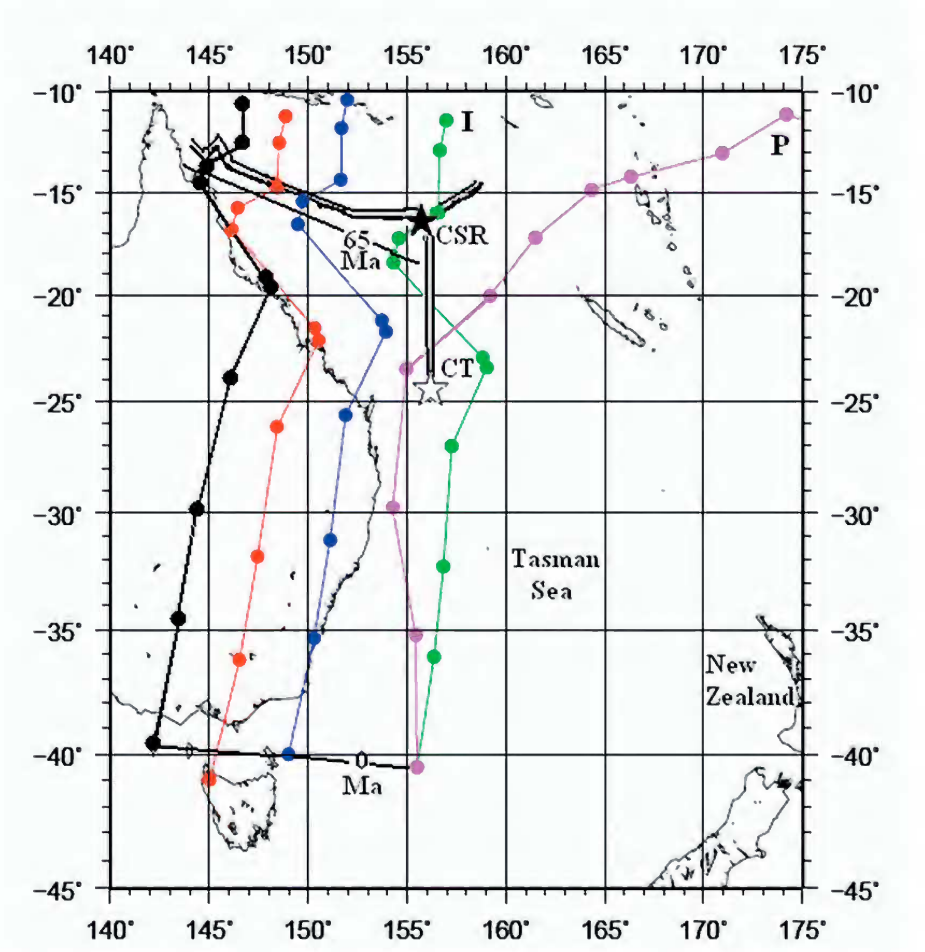

Figure 29 (preceding page). East Australia-Tasman Sea-Coral Sea plate motion tracks generated from present plume line array (Bass Strait-Western Tasman Sea). Tracks based on fixed Indian – Atlantic hotspots (I) are represented by black, red, blue and green lines with spots at 10 Ma intervals (0 – 100 Ma). The NW New South Wales central volcano line (~150o – 149o E, 30o – 34o S) lies adjacent to the blue line track. A Pacific hotspot track (P) is shown for comparison (pink line). The Coral Sea (CSR) – Cato Trough (CT) spreading rift system (double lines) indicates triple-point locations (black filled and unfilled stars respectively). Computer plot, Maria Seton.

Plume-driven NW New South Wales volcanism is only a strand within a broader plume system that erupted across moving eastern Australian lithosphere. An ultimate origin may lie within late Cretaceous Coral Sea rifting, with the original plumes now in dormant repose below the southern Bassian – Tasman basins.

ACKNOWLEDGEMENTS

The Linnean Society of New South Wales and organising committee for staging the 'Volcanoes of Northwest New South Wales' Natural History Field Symposium, Coonabarabran, 24 – 27 th September , 2018, and providing for publication of Symposium presentations. Dr Ben Cohen, University of Glasgow, Scotland and Dr Morrie Duggan, Braunstone, NSW, made substantial contributions of illustrative materials, and provided invaluable comments on the ms. Dr Michael Bruce, Petrology and Geochemistry, NSW Department of Planning, Industry and Environment, Sydney, made a constructive critique on the ms. Professor Ken McQueen, University of Canberra, ACT, and Ross Pogson, Geoscience, Australian Museum, Sydney, NSW, provided additional field and specimen photography. Professor Nick Rawlinson, Department of Earth Sciences, University of Cambridge, UK provided and gave permission to use seismic tomographic figures from his 2017 Geophysical Research Letter study. Dr Tracey Crossingham, School of Earth and Environmental Sciences, University of Queensland, Brisbane provided and permitted use of her Warrumbungle volcano PhD study. Terry Coldham, Gemmological Association of Australia, provided a map of the New England basalt fields. Joan Henley and The Geological Survey of New South Wales provided 1: 250 000 northern New England, NSW and SE Queensland map sheets in connecting areas. Simone Meekin, Geological Survey New South Wales and Larry Barron, Sydney, aided with literature search. Dr Maria Seton, Earth Sciences, Sydney University, provided Australian Plate movement modelling

REFERENCES

Abbott, M.J. (1969). Petrology of Nandewar Volcano, N.S.W., Australia. *Contributions to Mineralogy and Petrology* **20** (2), 115-134.

Barron, L.M., Barron, B.J., Mernagh, T.P. and Birch, W.D. (2008). Ultra high pressure macro diamonds from Copeton, (New South Wales, Australia), based on Raman spectroscopy of inclusions. *Ore Geology Reviews* **34**, 76 - 85.

Brown, R.E. and Stroud, W.J. (1997). *Inverell 1: 250 000 Metallogenic Map SH/56-5: Metallogenic study and Mineral Deposit Data Sheets*, 576pp. Geological Survey of New South Wales, Sydney.

Brown, R.E., Cranfield, L.C., Denaro, T.J., Burrows, P.E., Henley, H.F. and Brownlow, J.W. (2014). *Warwick-Tweed Heads Special metallogenic map SH/56-2 and SH/56-3*, Geological Survey of New South Wales, Maitland.

Bull, K.F. and Troedson, A.L. (2018). Permian pumice to Miocene Magmas: volcanology of Warrumbungle National Park. Program, Abstracts and Field Guide, 2018 Linnean Society of NSW Natural History Field Symposium, Coonabarabran 25th-27th September 2018, p 4.

Cameron, R.G.,Barron, L.M., Meakin,N.S., Warren, A.Y.E., Raymond, O.L., Morgan, E.J., Henderson, G.A.M. and Pogson, D.J. (1999). Cainozoic. In 'Dubbo 1: 250 000 Geological Sheets SI/55-4, 2nd edition. Explanatory Notes' (Compilers N.S. Meakin and E.J. Morgan) pp. 336-356. (Geological Survey of New South Wales: Sydney).

Carlton, A. and Bull K. (2018). Geophysical signatures of the Warrumbungle National Park. Volcanoes of North West New South Wales. Program, Abstracts and Field guide, 2018 Linnean Society of NSW Natural History Field Symposium, Coonabarabran 25th-27th September 2018, p 5.

Chan, R.A. (2003). Bathurst and Forbes 1: 250 000 Map Sheets, New South Wales. CRC LEME, Geoscience Australia, Canberra, 5pp.

Cohen, B.E. (2007).High- resolution $^{40}Ar/^{39}Ar$ geochronology of intraplate volcanism in eastern Australia. PhD thesis, School of Physical Sciences, University of Queensland, Brisbane.

Cohen, B.E., Knesel, K.M., Vasconcelos, P.M. and Schellart, W.P. (2013). Tracking Australian plate motion through the Cainozoic: Constraints from $^{40}Ar/^{39}Ar$ geochronology. *Tectonics* **32**, 1371-1383.

Cohen, B.E., Knesel, K.M., Vasconcelos , P.M., Theide, D.S. and Hergt, J.M. (2008). $^{40}Ar/^{39}Ar$ constraints on the timing and origin of Miocene leucitite volcanism in south eastern Australia. *Australian Journal of Earth Sciences* **55**, 407-418.

Crossingham, T.J. Ubide, T., Vasconcelos, P.M. and Mallmann, G. (2018). Parallel plumbing systems feeding a pair of co-eval volcanoes in eastern Australia. *Journal of Petrology* **59** (6), 1035 - 1066.

Crossingham, T.J., Vasconcelos, P.M., Cunningham, T. and Knesel, K.M. (2017). $^{40}Ar/^{39}Ar$ geochronology and volume estimates of the Tasmantid Seamounts: support for a change in motion of the Australian plate. *Journal of Volcanological and Geothermal Research* **343**, 95 - 108.

Cundari, A. (1973). Petrology of the leucite-bearing lavas in New South Wales. *Journal of the Geological Society of Australia* **20**, 456-492.

Cundari, A., Renard, J.G.R. and Gleadow, A.J.W. (1978). Uranium-potassium relationships and apatite fission-track ages for a differentiated leucitite suite from New South Wales (Australia). *Chemical Geology* **22**, 11-20

Davies, D.R., Rawlinson, N., Iffaldano, N. and Campbell, L.H. (2015). Lithospheric controls on magma composition along Earth's longest continental hotspot track. *Nature* **525**, 511-514.

Dawson, M.W., Spiller, F.C. P., Brownlow, J.W. and Barnes, R.G. (2003). Brigalow Belt South Bioregion geological map. Geological Survey of New South Wales, New South Wales Department of Mineral Resources, Sydney.

Duggan, M.B. (1988). Zirconium-rich sodic clinopyroxenes in felsic volcanics from the Warrumbungle Volcano, central New South Wales. *Mineralogical Magazine* **52**, 491-496.

Duggan, M.B. (1990). Wilkinsonite $Na_2 Fe^{2+}_4 Fe^{3+}_2 Si_6 O_{20}$, a new member of the aenigmatite group from the Warrumbungle volcano, New South Wales, Australia. *American Mineralogist* **75**, 694 -701.

Duggan, M.B. and Knutson, J. (1991). The Warrumbungle Volcano, central New South Wales. *Bureau Mineral Resources Record 1991/44*. Bureau of Mineral Resources, Canberra, ACT.

Duggan, M. B. and Knutson, J. (1993). *'The Warrumbungle Volcano: a geological guide to the Warrumbungle National Park'*. Australian Geological Survey Organisation, Canberra, ACT.

Duggan, M.B., Knutson, J. and Ewart, A. (1993). *'Warrumbungle, Nandewar and Tweed Volcanic Complexes' Excursion guide C4. IAVCEI Meeting, Canberra*. Australian Geological Survey Organisation, Canberra, ACT.

Edwards, J. (1988). Geology of the alkaline volcanic complex of the Canobolas Mountains, Orange, N.S.W. Hons Thesis, University of Melbourne.

Ewart, A. (1985). Aspects of the mineralogy and chemistry of the intermediate – silicic Cainozoic rocks of Eastern Australia. Part 2: Mineralogy and Petrogenesis. *Australian Journal of Earth Sciences* **32** (4), 383-413.

Ewart, A., Chappell, B.W. and Le Maitre, R.W. (1985). Aspects of the mineralogy and chemistry of the intermediate – silicic Cainozoic rocks of Eastern Australia. Part 1: Introduction and Geochemistry. *Australian Journal of Earth Sciences* **32** (4), 359-382.

Ewart, A.E., Chappell, B.W. and Menzies, M.A. (1988). An overview of the Geochemical and Isotopic Characteristics of the Eastern Australian Cainozoic Provinces. *Journal of Petrology, Special Lithospheric Issue*, pp 225-273.

Ghorbani, M.R. (1999). Petrology and Geochemistry of the Warrumbungle Volcano, New South Wales. PhD thesis, University of Sydney.

Ghorbani, M.R. (2003). Phonolitic and trachytic rocks from Warrumbungle volcano, different sources and conditions. *EGS-AGU Joint Assembly, Niece, France, 6 – 11 April 2003, abstract # 9241.*

Ghorbani, M.R. and Middlemost, E.A.K. (2000). Geochemistry of pyroxene inclusions from Warrumbungle Volcano. *American Mineralogist* **85**, 1349 – 1367.

Glen, R.A. (2013). Refining accretionary orogen models for the Tasmanides of eastern Australia. *Australian Journal of Earth Sciences* **60**, 315-370.

Glen, R.A. (2015). 'The Tasmanides of eastern Australia' (Eds A.P.M Vaughn, P.T. Leat and R.J. Pankhurst) pp. 23-96. *Geological Society of London Special Publication* **246**.

Hansma, J. and Tover, E. (2018). Paleomagmatism of mid- Miocene leucitite volcanics in eastern Australia. *Geophysics Journal International* **215**, 303 -313.

Holmes, K. W. B. (2018). The Mid Miocene flora preserved in the diatomite beds of the Chalk Mountain Formation, Warrumbungle Volcano complex. Program, Abstracts and Field guide, 2018 Linnean Society of NSW Natural History Field Symposium, Coonabarabran 25th-27th September 2018, p 8.

Higgins, K., Hashimoto, T., Rollet, N., Colwell, J., Hackney, R., & Milligan, P. (2015). Structural analysis of extended Australian continental crust: Capel and Faust Basins, Lord Howe Rise. In 'Sedimentary Basins and Crustal processes at Continental Margins: From Modern Hyper-extended Margins to and in Deformed Ancient Analogues' (Eds G.M. Gibson, F. Roure and G. Manatschal) pp. 9–33. *Geological Society of London Special Publication* **413**.

Irvine, T. N. and Baragar, W. R. A. (1971). A guide to the chemical classification of the common volcanic rocks. *Canadian Journal of Earth Sciences* **8**, 523–548.

Johnson, R. W., Compiler and Editor (1989). *'Intraplate Volcanism in Eastern Australia and New Zealand'* (Cambridge University Press: Cambridge).

Jones, I.M. (2018). Evolution and migration of Cenozoic Australia: Precision 40Ar/39Ar geochronology and geochemistry and paleomagnetic data from east Australia Cenozoic magmas. PhD thesis, School of Earth and Environmental Sciences. University of Queensland, Brisbane.

Jones, I., Verdel, C., Crossingham, T. and Vasconcelos, P. (2017). Animated reconstruction of the Late Cretaceous to Cenozoic northward migration of Australia and implications for the generation of east Australian mafic magmatism. *Geosphere* **13** (2), 1-22.

Kalnins, L.M., Cohen, B.E., Fitton, J.G., Mark, D.F., Richards, F.D. and Barfod, D.N. (2015). The East Australian, Tasmantid and Lord Howe Volcanic Chains: Possible mechanisms behind a trio of hot spot trails. Abstract D141A-2591. AGU Fall Meeting, 14–18 Dec., San Francisco.

Knesel, K.M., Cohen, B.E., Vasconcelos, P.M. and Theide, S.M. (2008). Rapid change in the drift of the Australian plate records collision with Ontong Java Plateau. *Nature* **454**, 754-757.

McDougall, I. and Wilkinson, J.F.G. 1967. Potassium-argon dates on some Cainozoic volcanic rocks from northeastern New South Wales. *Journal of the Geological Society of Australia* **14** (2), 225-233.

MacNevin, A.A. (1977). Diamonds in New South Wales. Department of Mines, Geological Survey of New South Wales, Mineral Resources **42**.

Matthews, K.J., Maloney, K.T., Zahirovic, S., Williams, S.E. and Müller (2016b). Global boundary evolution and kinematics since the late Palaeozoic. *Global and Planetary Change* **146**, 226-250.

McQueen, K.G., González, O.R., Roach, I.C., Pillans, B.J., Dunlap, W.J. and Smith, M.L. (2007). Landscape and regolithfeatures related to Miocene leucitite lava flows, El Capitan north east of Cobar, New South Wales. Australian Journal of Earth Sciences 54(1), 1-17.

Matthews, K.J., Seton, M. and Müller (2016a). A global scale reorganization event at 105 – 95 Ma. *Earth and Planetary Science Letters* **355-356**, 283-293.

Meyer, H.O.A., Milledge, H.J. and Sutherland, F.L. (1997). Unusual diamonds and unique inclusions from New South Wales, Australia. *Russian Geology and Geophysics* **38** (2), 305 – 331.

Middlemost, E.A.K. (1981). The Canobolas Complex, N.S.W., an alkaline shield volcano. *Journal of the Geological Society of Australia* **28** (1-2), 33 – 49.

Middlemost, E.A.K. (2013). 'Magmas, Rocks and Planetary Development: A Survey of Magma/Igneous rock Systems', Chapter 10.8, p. 220. Routledge, London and New York.

Nekvasil, H., Dondolini, A., Horn, J., Filberto, H. and Lindsley, D.H. (2004). The Origin and Evolution of Silica-saturated Alkalic Suites: an experimental study. *Journal of Petrology* **45** (4), 693 -721.

Oostingh , K.F., Jourdan, F., Merle, R. and Chiardia, M. (2015). Spatio-temporal geochemical evolution of the SE Australian upper mantle deciphered from the Sr, Nd and Pb isotope compositions of Cenozoic intraplate volcanic rocks. *Journal of Petrology* **57**(8), 1509-1530.

Pogson D.J. and Watkins, J.J. (1998). Bathurst 1: 250 000 Geological Sheet SI/55-8: Explanatory Notes, CAINOZOIC, pp. 271-282. Geological Survey New South Wales, Sydney.

Rawlinson, N., Davies, D.R. and Pilia, S. (2017a). The mechanisms underpinning Cenozoic intraplate volcanism in eastern Australia: Insights from seismic tomography and geodynamic modelling. *Geophysical Research Letters* **44**, 9681-9690.

Rawlinson, N., Davis, D.R. and Pilia, S. (2017b). Supporting information for the "The mechanisms underpinning Cenozoic intraplate volcanism in eastern Australia from seismic tomography and geodynamic modelling". Grl 56337-supp-001-supplementary pdf, 1-14.

Richards, F.D., Kalnins, L.M., Watts, A.B., Cohen, B.E., and Beaman, R.J. (2018). The Morphology of the Tasmantid Seamounts: Interactions between tectonic inheritance and magmatic evolution. *Geochemistry, Geophysics, Geosystems* **19**, 3870- 3891.

Shao, F., Nui, Y., Regelous, M. and Zhu, D-C. (2015). Petrogenesis of peralkaline rhyolites in an intraplate setting: Glass House Mountains, southeast Queensland, Australia. *Lithos* **216-217**, 196-210.

Stolz, A.J. (1985). The Role of Fractional Crystallization in the evolution of the Nandewar Volcano, North-eastern New South Wales, Australia. *Journal of Petrology* **26** (4), 1002-1026.

Stolz, A.J. (1986). Mineralogy of the Nandewar Volcano, northeastern New South Wales. *Mineralogical Magazine* **50**, 241-255.

Sutherland, F.L. (1981). Migration in relation to possible tectonism and regional controls in eastern Australian volcanism. *Journal of Vocanology and Geothermal Research* **9**, 181-213.

Sutherland, F.L. (1993). Late thermal events based on zircon fission track ages in northeastern New South Wales and southeastern Queensland. Links to Sydney Basin Seismicity? *Australian Journal of Earth Sciences* **40**, 461- 470.

Sutherland, F. L. (1995). '*The Volcanic Earth*'. UNSW Press, Sydney.

Sutherland, F.L. (2003). 'Boomerang' migratory intraplate volcanism, eastern Australian rift margins and Indian-Pacific mantle boundary. *Geological Society of Australia Special publication* **22** and *Geological Society of America Special Paper* **372**, 203-221.

Sutherland, F.L. (2011). Diversity within geodiversity, underpinning habitats in New South Wales. *Proceedings of the Linnean Society of New South Wales* **132**, 37-54.

Sutherland, F.L., Graham, I.T., Zwingmann, H., Pogson, R.E. and Barron , B.J. (2005).Belmore Volcanic province , northeastern New South Wales, and some implications for plume variations along Cenozoic migratory trails. *Australian Journal of Earth Sciences* **52**, 897-919.

Sutherland, F.L., Barron, B.J., Colchester, D.M. and McKinnon, A.R (2007). Unusual baryte-bearing hybrid basalt, Bourke-Byrock area, northern New South Wales. *Journal & Proceedings of the Royal Society of New South Wales* **140**, 27-46.

Sutherland, F.L., Graham, I.T., Meffre, S., Zwingmann, H. and Pogson, R.E. (2012). Prolonged passive margin volcanism, East Australian Plate: outbursts, progressions, plate controls and suggested causes. *Australian Journal of Earth Sciences* **57**, 983-1005.

Sutherland, F.L., Graham, I.T., Hollis, J.D., Meffre, S., Zwingmann, H., Jourdan, F. and Pogson, R.E. (2014).

Multiple felsic events within post-10 Ma volcanism, Southeast Australia: inputs in appraising proposed magmatic models. *Australian Journal of Earth Sciences* **61**, 241-267.

Thompson, P. (2018). Field observations of cobble and boulder stream deposits from the erosion of the Warrumbungle Volcano. Program, Abstracts and Field guide, 2018 Linnean Society of NSW Natural History Field Symposium, Coonabarabran 25th-27th September 2018, p 10.

Tomkins, K.M. and Hesse, P.P. (2004). Evidence of Late Cenozoic uplift and climate changein the stratigraphyof the Macquarie River valley, New South Wales. *Australian Journal of Earth Sciences* **51**, 273-290.

Troedson, A.L. and Bull, K.F. (2018). A new geology map of Warrumbungle National Park and environs. Program, Abstracts and Field guide, 2018 Linnean Society of NSW Natural History Field Symposium, Coonabarabran 25th-27th September 2018, p 5.

Tulau, M.J., McInnes-Clark, S. and Morand, D. (2018). Mass movements in Warrumbungle National Park, NSW. Program, Abstracts and Field guide, 2018 Linnean Society of NSW Natural History Field Symposium, Coonabarabran 25th-27th September 2018, p 11.

Vickery, N.M., Dawson, Sivell, W.J., Malloch, K.R. and Dunlap, W.J. (2007) Cainozoic igneous rocks in the Bingera to Inverell area, northeastern New South Wales. *Quarterly Notes of the Geological Survey of New South Wales* **123**, 1 – 31.

Ward, C.R. and Kelly, B.F.J. (2013). Background Paper on the New South Wales Geology, with a focus on Basins Containing Coal Seam Gas Resources, for the office of the NSW Chief Scientist and Engineer. UNSW Global, Australia, 28 August 2013. www.Chief.scientist.nsw.gov.au/_data/assets/pdf_file/009/31788/NSW - Geology- Background Paper Ward-and Kelly-unsw.pdf

Wellman, P. (1986). Intrusions beneath large alkaline intraplate volcanoes. *Exploration Geophysics* **17,** 30-35.

Whitaker, M.L., Nekvasil, H., Lindsley, D.H. and Difranesco, N.J. (2007). The role of pressure in in producing compositional diversity in intraplate basaltic magmas. *Journal of Petrology* **48** (2), 365 – 393.

Whitehead, J. (2014). '*The Geology of the Warrumbungle Range*'. 2nd Edition. Whitehead, John, Coonabarabran, NSW.

Wilkinson, J.F.G. (1975). Ultramafic inclusions and high pressure megacrysts from a nephelinite sill, Nandewar Mountains, north-eastern New South Wales, and their bearing on the origin of certain ultramafic inclusions in alkaline volcanic rocks. *Contributions to Mineralogy and Petrology* **51**, 235-262.

Wilkinson, J.F.G. (1977). Analcime phenocrysts in a vitrophric analcimite – primary or secondary? *Contributions to Mineralogy and Petrology* **64**, 1-10.

Zhang, M. and O'Reilly, S.Y. (1997). Multiple sources for basaltic rocks from Dubbo, eastern Australia: geochemical evidence for plume – lithospheric interaction. *Chemical Geology* **136**, 33-54.